Development/Plasticity/Repair

The Loop Diuretic Bumetanide Blocks Posttraumatic p75^{NTR} Upregulation and Rescues Injured Neurons

Anastasia Shulga,[1,2,3] **Ana Cathia Magalhães,**[1,2] **Henri Autio,**[2] **Stefan Plantman,**[4] **Antonio di Lieto,**[2] **Anders Nykjær,**[5] **Thomas Carlstedt,**[6] **Mårten Risling,**[4] **Urmas Arumäe,**[1] **Eero Castrén,**[2] and **Claudio Rivera**[1,2,7]

[1]Institute of Biotechnology, [2]Neuroscience Center, and [3]Department of Neurological Sciences, University of Helsinki, FI-00014 Helsinki, Finland, [4]Department of Neuroscience, Karolinska Institutet, SE-171 77 Stockholm, Sweden, [5]The Lundbeck Foundation Research Center MIND, Department of Medical Biochemistry, Aarhus University, DK-8000C Aarhus, Denmark, [6]Department of Hand Surgery, Karolinska Institutet, Södersjukhuset, SE-118 83 Stockholm, Sweden, and [7]Université de la Méditerranée, UMR S901 Aix-Marseille 2, Institut de Neurobiologie de la Méditerranée, 13009 Marseille, France

Injured neurons become dependent on trophic factors for survival. However, application of trophic factors to the site of injury is technically extremely challenging. Novel approaches are needed to circumvent this problem. Here, we unravel the mechanism of the emergence of dependency of injured neurons on brain-derived neurotrophic factor (BDNF) for survival. Based on this mechanism, we propose the use of the diuretic bumetanide to prevent the requirement for BDNF and consequent neuronal death in the injured areas. Responses to the neurotransmitter GABA change from hyperpolarizing in intact neurons to depolarizing in injured neurons. We show *in vivo* in rats and *ex vivo* in mouse organotypic slice cultures that posttraumatic GABA$_A$-mediated depolarization is a cause for the well known phenomenon of pathological upregulation of pan-neurotrophin receptor p75^{NTR}. The increase in intracellular Ca^{2+} triggered by GABA-mediated depolarization activates ROCK (Rho kinase), which in turn leads to the upregulation of p75^{NTR}. We further show that high levels of p75^{NTR} and its interaction with sortilin and proNGF set the dependency on BDNF for survival. Thus, application of bumetanide prevents p75^{NTR} upregulation and neuronal death in the injured areas with reduced levels of endogenous BDNF.

Introduction

While intact mature central neurons do not require brain-derived neurotrophic factor (BDNF) for survival (Giehl et al., 2001; Li et al., 2008; Shulga et al., 2008; Rauskolb et al., 2010), under pathophysiological conditions neuronal populations become dependent on the trophic support provided by BDNF (Klöcker et al., 2000; Schäbitz et al., 2000; Giehl et al., 2001; Shulga et al., 2008, 2009). However, supplying the affected neurons with this trophic factor *in vivo* has proven to be technically extremely challenging (Thoenen and Sendtner, 2002), and novel strategies are needed to circumvent this problem.

The mechanism of posttraumatic dependency on BDNF is not clear. BDNF signaling is mediated through two receptors, TrkB and neurotrophin receptor p75 (p75^{NTR}). The signaling of the latter has been frequently associated with cell death (Huang and Reichardt, 2001). Trauma is well known to increase the level of p75^{NTR} expression in neurons and glia (Chao, 2003). Apart from

promoting cell death, high p75^{NTR} levels increase the affinity and specificity of Trk receptors to their cognate ligands (Huang and Reichardt, 2001; Chao, 2003); this could enhance the trophic efficiency of available BDNF. Thus, we hypothesized that, after trauma, the fate of the cell could depend on the balance between BDNF survival-promoting signaling through TrkB and the opposing signaling of p75^{NTR}. High levels of p75^{NTR} expression in axotomized neurons could set the requirement for BDNF trophic support, leaving the survival outcome at the mercy of the accessibility of endogenous BDNF. If this is the case, discovering the way to prevent pathological p75^{NTR} upregulation would provide the possibility for the development of novel therapeutic strategies.

Although downstream signaling, processing, and function of p75^{NTR} is a subject of intense investigation (Underwood and Coulson, 2008), much less is known about the regulation of p75^{NTR} expression in nontraumatic (Gao et al., 2007) and traumatic (Dubreuil et al., 2003; Peterson and Bogenmann, 2003; Ramos et al., 2007) conditions. p75^{NTR} is widely expressed in the developing CNS, downregulated in the adult brain, and reexpressed after injury (Underwood and Coulson, 2008). Interestingly, the changes in the expression level of p75^{NTR} are paralleled by functional changes in the GABAergic inhibitory neurotransmission: the developmental and posttraumatic shifts in GABA$_A$ receptor-mediated responses (Blaesse et al., 2009). GABA-induced responses are depolarizing and able to induce intracellular Ca^{2+} ([Ca^{2+}]$_i$) increase during development, but become hyperpolarizing in mature neurons due to the upregulation of K$^+$–Cl$^-$ cotransporter KCC2 (Blaesse et al., 2009). After trauma, GABA$_A$-mediated responses become again depolarizing due to

functional downregulation of KCC2 and accumulation of intracellular Cl^- through the activity of $Na^+–K^+–2Cl^-$ cotransporter NKCC1 (Nabekura et al., 2002; Blaesse et al., 2009). In this context, an interesting question arises: Are parallel changes in $p75^{NTR}$ expression and the shift in polarity of $GABA_A$-mediated responses interrelated?

Using *in vivo* and *ex vivo* models, we show that $GABA_A$-mediated $[Ca^{2+}]_i$ increase is essential for the posttraumatic upregulation of $p75^{NTR}$. We also show that the induction of $p75^{NTR}$ expression renders injured neurons dependent on the trophic support by BDNF. Diuretic drug bumetanide is a specific inhibitor of NKCC1 (Blaesse et al., 2009), and thus it is able to prevent the posttraumatic shift in the polarity of GABA-evoked responses. We show that, through this action, bumetanide prevents the upregulation of $p75^{NTR}$ and consequent neuronal death, and suggest bumetanide as a novel therapeutic strategy for the injured neurons.

Materials and Methods

Organotypic slice cultures

Hippocampal slices from 8- to 9-d-old male and female NMRI mice were prepared according to the method by Stoppini et al. (1991). Transverse 350-μm-thick slices were cut from the hippocampi with a McIlwain tissue chopper. They were immediately placed on sterile Millicell-CM membranes (Millipore) in six-well culture trays with 1 ml of plating medium (Neurobasal, with B27 supplement; Invitrogen) containing antibiotic (Primocin; InvivoGen). Slices were kept at 37°C under 5% CO_2 in air. One day after plating, the medium was changed for antibiotic-free medium and renewed again 4 d after plating.

Ex vivo *axotomy model*

All experiments were performed 4 d after plating. A lesion between CA3 and CA1 regions was made using a piece of a razor blade (cutting edge, 4 mm) under light stereomicroscope. The lesion traverses the whole slice thickness in the vertical direction, completely separating CA3 and CA1; the dentate gyrus region is not affected, and the slice is not cut into two pieces (see Fig. 1a). We have previously reported that unlesioned slices of this age possess GABA- and BDNF-evoked responses characteristic for the intact mature nervous tissue, and that this *ex vivo* axotomy model gives similar results as observed in the *in vivo* axotomy model (Shulga et al., 2008). TrkB-Fc (recombinant human TrkB-Fc chimera; 200 ng/ml; R&D Systems), Fc (human IgG Fc fragment; 230 ng/ml; Millipore), bumetanide (10 μM; Tocris), Rex antibody (1:250; a kind gift from Dr. Louis Reichardt, University of California, San Francisco, San Francisco, CA), antibody to p75 ECD (1:500 for function blocking; AB1554; Millipore), plasmin (45 nM; American Diagnostica), antibodies to proNGF and proBDNF (1:100; Alomone Labs), BAPTA-AM (100 μM; Invitrogen; was added to the medium and loaded three times on top of the slices every 10 min; thereafter, slices were transferred to the medium without BAPTA-AM), TTX (2 μM; Tocris), KCl (10 mM), Ni^{2+}/Cd^{2+} (100 μM), muscimol (50/100 μM; Tocris), bicuculline (20 μM; Sigma-Aldrich), 4-aminopyridine (4-AP) (100 μM; Tocris), nimodipine (20 μM; Tocris), and (1*R*,4*r*)-4-((*R*)-1-aminoethyl)-*N*-(pyridin-4-yl)cyclohexanecarboxamide (Y-27632) (100 μM; Sigma-Aldrich) were added to slices immediately after the lesion procedure; unlesioned slices were treated at the same time. All slices were collected for analyses 1 d after the experiment, unless stated otherwise in the text.
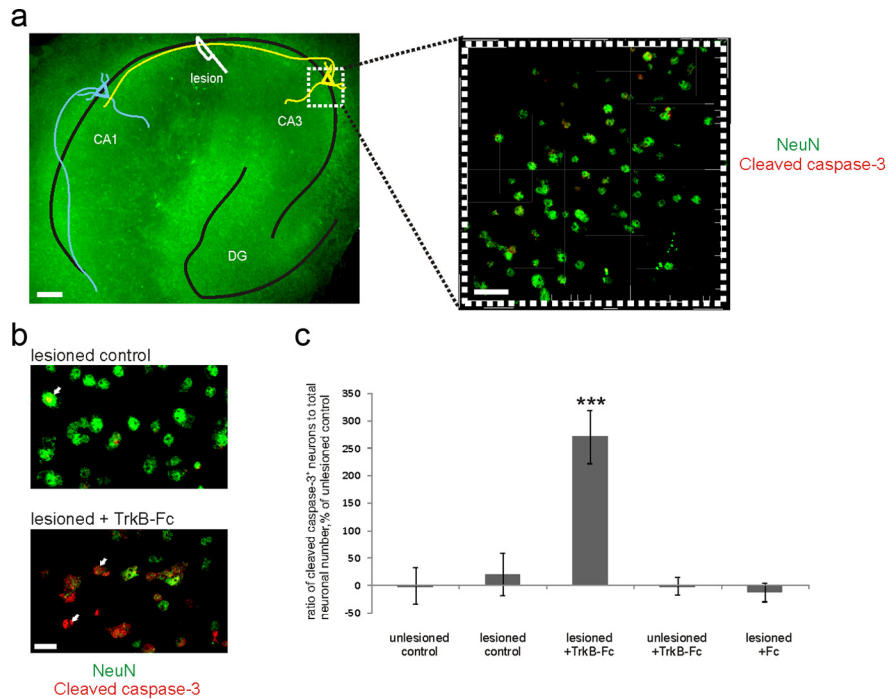

Figure 1. Axotomy induces the trophic requirement for endogenous BDNF. *a*, *Ex vivo* axotomy model. Left, Representative fluorescent picture of a lesioned slice stained immunohistochemically for NeuN. Schematic drawing: CA3 neurons (yellow) are axotomized and CA1 neurons (blue) are denervated. Scale bar, 100 μm. Right, A representative confocal image taken from the middle of CA3 region for the stereological counting of neurons. Scale bar, 20 μm. *b*, Zoomed parts of confocal images from the CA3 region of the lesioned slices with and without TrkB-Fc (the scavenger of the endogenous BDNF) stained immunohistochemically for NeuN (green) and cleaved caspase-3 (red). White arrows, Cleaved caspase-3-positive neurons. Scale bar, 10 μm. *c*, Ratio of cleaved caspase-3-positive (=apoptotic) neuronal number to total neuronal number obtained by blind stereological counting, percentage of unlesioned control ratio value. Deprivation of endogenous BDNF with TrkB-Fc causes significant increase in apoptotic neuronal number in the lesioned, but not unlesioned, slices at 1 d after the injury. Control human Fc fragment had no effect. $n = 50$ slices/4880 neurons; ***$p < 0.001$, one-way ANOVA and Bonferroni's *post hoc* analyses. Error bars indicate SEM.

In vivo *axotomy*

All animal experiments were approved by the Local Ethics Committee for Animal Research at the University of Helsinki. Adult male Wistar rats (240–330 g) were used. One hour before the surgery, rats received an intraperitoneal injection of bumetanide (30 mg/kg; Tocris; diluted in saline containing 0.25% NaOH). Control animals received an intraperitoneal injection of saline at the same time. Animals were anesthetized with isoflurane. A hemilaminectomy was performed at the lumbar L4–L6 region of the spinal cord. The dura was opened, and the corresponding L4–L6 ventral roots were identified under microscopic control, isolated, and rhizotomized with fine microscissors. The divided roots were then left in the spinal canal. The wounds were closed with sutures. After surgery, the animals were allowed to survive for 3 d and then perfused with 4% paraformaldehyde. The final identification of rhizotomized spinal cord segments was performed in each animal after fixation. Spinal cords were postfixed for 24 h and submerged in 30% sucrose in PBS; thereafter, 14 μm cryosections were prepared and stained immunohistochemically.

Knock-out animals

Pups were used from a mouse line with disruption in the *Slc12a2* gene encoding the Na^+-K^+-$2Cl^-$ cotransporter isoform 1 (NKCC1) (Pace et al., 2000). Genotyping was performed on tail biopsy DNA by PCR using standard protocols (Pfeffer et al., 2009). Sortilin-deficient and wild-type parental mice were genotyped as described previously (Jansen et al., 2007). $p75^{+/+}$ and $p75^{-/-}$ mice (Lee et al., 1992) were perfusion-fixed with 4% paraformaldehyde, postfixed for 24 h, and submerged in 30% sucrose in PBS; thereafter, 50 μm cryosections were prepared and stained immunohistochemically according to the same protocol as organotypic hippocampal slices (see below).
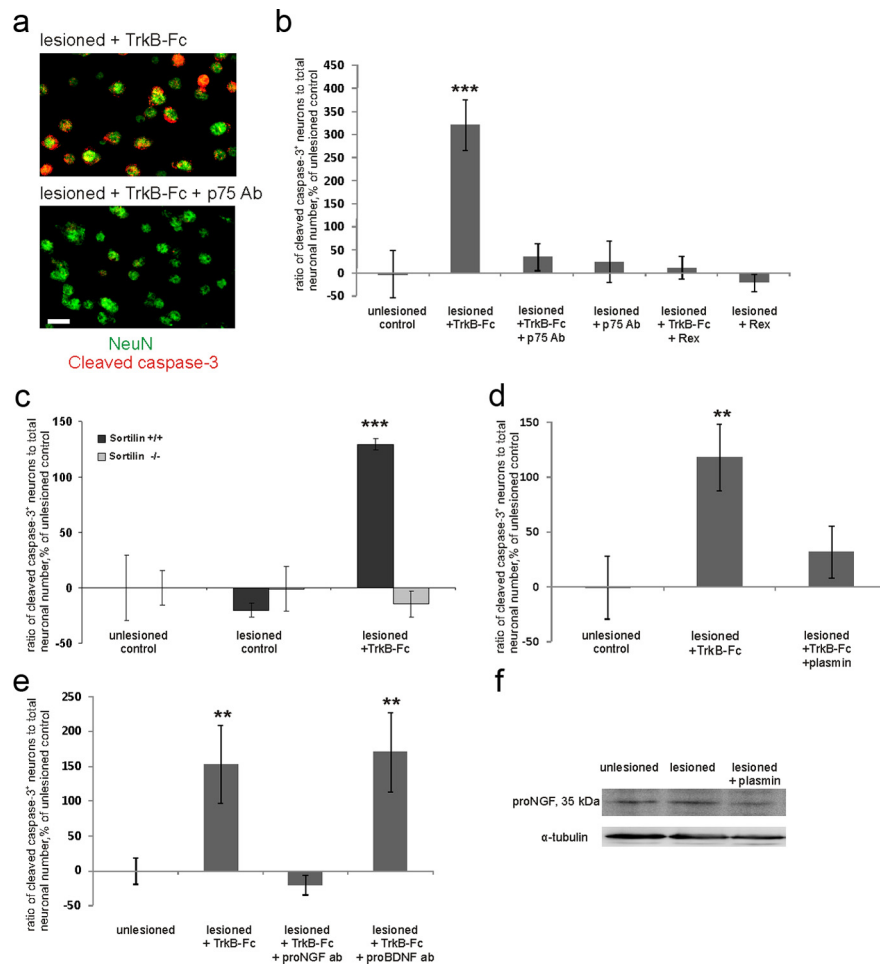
Figure 2. Posttraumatic emergence of the requirement for BDNF is caused by p75 NTR. **a**, Images of axotomized TrkB-Fc-treated neurons with and without p75 NTR-blocking antibodies obtained similarly to those in Figure 1b. Scale bar, 10 μm. **b**, Ratio of cleaved caspase-3-positive (=apoptotic) neuronal number to total neuronal number obtained by blind stereological counting, percentage of unlesioned control ratio value. Treatment with two different function-blocking antibodies directed against the extracellular domain of p75 NTR [p75 Ab; AB1554; Millipore; and Rex (Weskamp and Reichardt, 1991)] abolished the increase in the number of apoptotic neurons promoted by TrkB-Fc. $n = 46$ slices/4750neurons; ***$p < 0.001$, one-way ANOVA and Bonferroni's *post hoc* analyses. **c**, TrkB-Fc treatment did not induce caspase activation in sortilin knock-out mice. Quantification was performed as in **b**; $n = 48$ slices/4600 neurons; ***$p < 0.001$, one-way ANOVA and Bonferroni's *post hoc* analyses. **d**, Treatment with plasmin abolished the TrkB-Fc-induced increase in the number of apoptotic neurons. Quantification was performed as in **b**; $n = 33$ slices/3350 neurons; **$p = 0.017$, one-way ANOVA and Bonferroni's *post hoc* analyses. **e**, Treatment with antibodies toward proNGF completely prevented TrkB-Fc-induced death induction, whereas antibodies toward proBDNF had no effect. $n = 41$ slices/3420 neurons; **$p = 0.05$, one-way ANOVA and Bonferroni's *post hoc* analyses. **f**, Western blot analyses with the antibody to proNGF. proNGF expression was upregulated by lesion and diminished by plasmin. $n = 3$ experiments/36 slices; **$p = 0.041$, one-way ANOVA and Bonferroni's *post hoc* analyses. For full image of the representative blot, see Figure 3a. Error bars indicate SEM.

Basal forebrain primary cultures

Rat embryonic septa were dissected on embryonic day 17. The meninges were carefully removed, and the tissue was incubated in papain solution for 10 min before trituration by pipetting. The cells were plated at the density of 200,000 cells/well on poly-L-lysine-coated coverslips in 24-well culture plates. The neurons were cultured in Neurobasal medium (Invitrogen) containing 1% penicillin–streptomycin, 1% L-glutamine, and 2% B27 supplement (Invitrogen). One-third of the medium was changed on day 3 after plating. On day 7 *in vitro*, the cells were treated overnight with proNGF (1 ng/ml) or proBDNF (5 ng/ml) in the absence or presence of antibodies against proNGF or proBDNF (1:100). The following day, the neurons were rinsed with PBS and fixed 15 min with 4% paraformaldehyde (PFA) solution.

Immunohistochemistry

Organotypic slice cultures. Slices remained on the Millicell-CM membranes during the whole staining procedure. They were fixed in 4% PFA overnight at 4°C. Thereafter, the slices were washed in PBS and dehydrated through a graded series of methanol in PBS (30, 50, 80%). Next, the slices were incubated in Dent's fixative (80% methanol, 20% DMSO; Sigma-Aldrich), washed in TBSTD (TBS, 0.1% Tween, 5% DMSO), and placed in 5% bovine serum albumin (BSA) (Sigma-Aldrich) plus 0.4% sheep serum (Sigma-Aldrich) in TBSTD overnight at 4°C. Thereafter, slices were incubated with primary antibodies diluted in the blocking solution at 4°C for 48 h. Rabbit anti-p75NT ECD Ab (1:500; AB1554; Millipore), mouse anti-NeuN Ab (1:400; Millipore), rabbit anti-cleaved caspase-3 Ab (1:200; Cell Signaling Technology), rabbit anti-p-cofilin (1:100; Santa Cruz Biotechnology), and goat anti-cleaved caspase-6 (1:100; Santa Cruz Biotechnology) were used. After washing in TBSTD, slices were incubated overnight with Alexa Fluor 488-conjugated donkey anti-mouse or rabbit IgG, Alexa Fluor 568-conjugated goat anti-rabbit or goat IgG (1:400; Invitrogen), and Cy5-conjugated donkey anti-mouse IgG (1:400; Jackson ImmunoResearch Laboratories). Slices were then washed in TBSTD, incubated in Hoechst (1:1000; Invitrogen), rinsed with TBSTD, and mounted with membranes on Superfrost Plus slides in Pro-Long Gold mounting medium (Invitrogen).

Basal forebrain primary cultures. After the fixation, coverslips were washed with PBS, treated with 0.2% Triton X-100 in PBS (TXP), and incubated in 10% sheep serum in TXP. Neurons were left in chicken anti-ChAT antibody (1:200; Abcam) in 10% sheep serum in TXP overnight at +4°C, washed with TXP, and incubated with Alexa Fluor 568-conjugated goat anti-chicken IgG (1:400; Invitrogen) in TXP at room temperature. Coverslips were then washed in TXP containing Hoechst (1:1000; Invitrogen), rinsed in MilliQ water, and mounted with ProLong Gold antifade reagent (Invitrogen).

Cryosections from ventral root axotomized rats. Sections were allowed to melt in the room temperature, washed in PBS, and incubated with 5% BSA. Thereafter, sections were incubated overnight with primary antibodies [p75 NTR: 1:500; Millipore; MAB365; NeuN: 1:400; Millipore; KCC2 (Ludwig et al., 2003): 1:500; cleaved caspase-3: 1:600; Cell Signaling Technology] in 5% goat serum, 5% BSA, and 0.3% Triton X-100 in PBS. The next day, sections were washed in PBS and incubated with secondary antibodies (Alexa Fluor 568-conjugated goat anti-rabbit or anti-mouse and Alexa Fluor 488-conjugated donkey anti-mouse or anti-rabbit; 1:400; Invitrogen) diluted in 0.3% Triton X-100 in PBS. Thereafter, sections were washed in PBS and mounted with ProLong Gold antifade reagent (Invitrogen).

Image acquisition and analyses

Image stacks consisting of 11 images from 10 and 20 μm below the organotypic slice surface were taken with a Leica TCS SP5 confocal microscope (Leica Microsystems) with an HC PL APO 20×, 0.7 NA objective using glycerol immersion, with zoom factor 4.5–5. Two image stacks were taken from each slice, one from the middle of the CA3 and the other from the middle of the CA1 region (see Fig. 1a, left). Three-dimensional reconstruction images from the stacks were analyzed in Bitplane Imaris software. Image stacks had a volume of 155 × 155 × 10 μm, the majority

of the 3D images containing 70–160 neurons (see Fig. 1a, right). Background extraction was performed blindly and in a similar way for every 3D image, using the image histogram. For the analysis of cleaved caspase-3 or -6-positive neurons, isosurface tool in Imaris software was used to mask the caspase-3 or -6 channel with NeuN channel to visualize only the neuronal cells. Neurons that had cleaved caspase-3 or -6 staining colocalizing with the NeuN-defined nucleus were considered as positive. For the analysis of $p75^{NTR}$-positive neurons, InMotion tool and a high-magnification factor in Imaris software were used for enhanced detail visibility. Neurons that had $p75^{NTR}$ staining around a NeuN-defined nucleus were considered as positive. The amount of $p75^{NTR}$-positive or cleaved caspase-3-positive neurons and the total number of neurons were analyzed by blind manual stereological counting, and the ratio was calculated.

For the analyses of p-cofilin immunostaining of organotypic slices and ChAT immunostaining of basal forebrain primary cultures, fluorescence images were acquired with Olympus BX61 microscope using 4, 10, or 20× objectives. For the analysis of immunostaining of cryosections from the ventral root axotomized rats, fluorescence images were acquired with Olympus BX61 microscope using 10 or 20× objectives. For the analysis of $p75^{NTR}$, total amount of $p75^{NTR}$-positive neurons for each animal from four sections per animal was counted by blind stereological counting. Total amount of neurons (identified by NeuN) was counted from each animal from four sections consecutive to each $p75^{NTR}$-stained section, and total $p75^{NTR}$-positive neuronal number was divided by total NeuN-positive neuronal number for each animal. Criteria for analysis were area of min 3900 arbitrary units (for the images taken with 10× objective) in ImagePro software (corresponding to ca 600 μm^2) to identify the motoneurons, and the density of $p75^{NTR}$ or cleaved caspase-3 staining of min 13 arbitrary units. For the analysis of KCC2, KCC2 immunostaining intensity was measured from each neuron in ImagePro software (selection criteria as above, identified by double staining with NeuN) and the average for each section was quantified.

Western blotting

Slices were homogenized in homogenization buffer (0.3 M sucrose, 10 mM HEPES, 1 mM EDTA, pH 7.2, containing protease inhibitors; Complete Mini; Roche) and incubated with Laemmli loading buffer for 45 min at 45°C. The solution was separated in 8–15% SDS-PAGE and electrophoretically transferred to nitrocellulose membranes. Blots were probed with antibody 9651 to $p75^{NTR}$ (Huber and Chao, 1995) (1:2000), proNGF (1:500; Alomone Labs), phospho-Akt Ser73 (1:2000; Cell Signaling Technology), pan-Akt (1:1000; Cell Signaling Technology), KCC2 (Ludwig et al., 2003) (1:2000), phosphotyrosine (clone 4G10; 1:1000; Millipore), or NKCC1 (T4; Developmental Studies Hybridoma Bank; 1:500), and developed using ECL-plus kit (GE Healthcare). After that, membranes were stripped using DTT/SDS in Tris-HCl, pH 7.0, and probed with mouse anti-mNGF (Millipore; 1:200), mouse anti-α-tubulin Ab (Sigma-Aldrich; 1:2000), or rabbit anti-β-tubulin (Covance; 1:3000). Optical densities of the bands were analyzed with the AIDA imaging software.
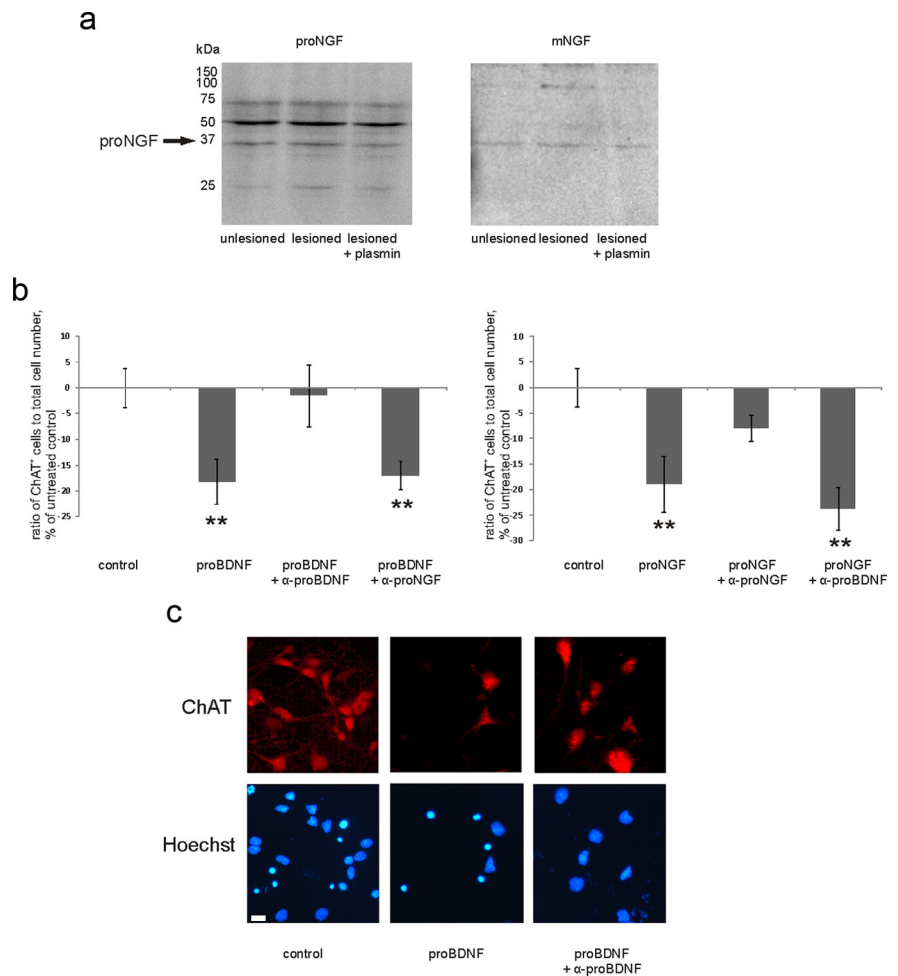

Figure 3. **a**, Representative Western blot with antibody to proNGF (left), reblotted with the antibody to mature NGF (right). Band row at 35 kDa is recognized by both antibodies, which verifies it as proNGF. For quantification, see Figure 2f. **b**, To verify the function-blocking specificity of antibodies to proNGF and proBDNF, we applied proNGF and proBDNF in the absence or presence of antibodies to proNGF and proBDNF to basal forebrain primary cultures (for details, see Materials and Methods). Each antibody specifically diminished the reduction in the number of ChAT-positive neurons induced by its cognate proneurotrophin, not having an effect on the response to another proneurotrophin. **p = from left to right: 0.027, 0.046, 0.015, 0.001, one-way ANOVA and Bonferroni's *post hoc* analyses; *n* = 5670 cells. Scale bar, 10 μm. **c**, Representative pictures from the experiment described in **b**. Error bars indicate SEM.

Immunoprecipitation

GammaBind G-Sepharose (GE Healthcare) was blocked with 5% milk, 1% BSA in PBS overnight and incubated with KCC2 antibody (Ludwig et al., 2003) (or rabbit serum for negative control) overnight at +4°C. Slices were homogenized in RIPA buffer (150 mM NaCl, 1% Triton-X, 0.5% DOC, 0.1% SDS, 50 mM Tris, pH 8) containing protease and phosphatase inhibitors (Complete Mini and PhosSTOP; Roche). One milligram of protein in 1 ml of RIPA was preclarified by G-Sepharose and then incubated with KCC2 antibody (Ludwig et al., 2003) attached to G-Sepharose overnight at +4°C. Sepharose beads were washed with RIPA buffer and eluted in 30 μl of Laemmli buffer, heated 5 min at +95°C. The supernatants were loaded to 8% SDS-PAGE gel and separated by standard Western blot protocol described above.

Real-time PCR

Total RNA was isolated with RNeasy kit (QIAGEN) and reverse transcribed with SuperScript III RNase H-Reverse Transcriptase (Invitrogen). cDNA samples were amplified using iQ SYBR Green Supermix (Bio-Rad) and detected with the Bio-Rad CFX96 real-time PCR detection system. Primers were designed on PrimerQuest software and tested with OligoAnalyzer software (eu.idtdna.com) and contained an intronic sequence in between. Sequences were as follows: AGGGCACATACTCAGATGAAGCCA ($p75^{NTR}$ FW), GGGCGTAGACCTTGTGATCCAT ($p75^{NTR}$ RW), CTCCGCTTTCATGTAGAGGAAG (Pgk1 FW), and
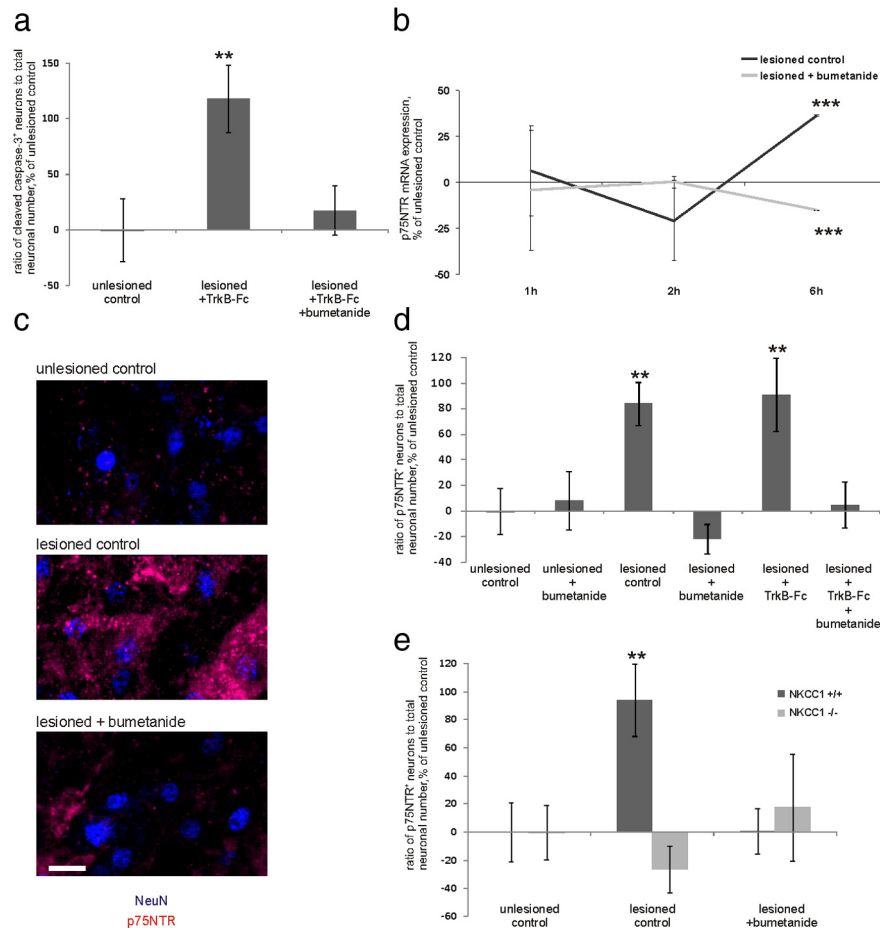
Figure 4. The NKCC1-blocking drug bumetanide prevents the posttraumatic emergence of requirement for BDNF and blocks the postaxotomy upregulation of p75 ^{NTR}. ***a***, Bumetanide abolishes the posttraumatic cell death induction in neurons deprived of BDNF by TrkB-Fc application. $n = 33$ slices/3350 neurons; $**p = 0.021$, one-way ANOVA and Bonferroni's *post hoc* analyses. ***b***, Quantification of real-time PCR analyses for p75 ^{NTR} mRNA, percentage of unlesioned control, at 1, 2, and 6 h after axotomy. At 6 h after axotomy, p75 ^{NTR} mRNA was upregulated, but not in the presence of bumetanide. $n = 72$ slices; $***p < 0.001$, one-way ANOVA and Bonferroni's *post hoc* analyses. ***c***, Fragments of representative confocal images from the CA3 region of unlesioned, lesioned, and lesioned bumetanide-treated slices stained immunohistochemically for NeuN (blue) and p75 ^{NTR} (red). Scale bar, 10 μm. ***d***, Ratio of p75 ^{NTR}-positive neuronal number to total neuronal number, obtained by blind stereological counting in the CA3 region, percentage of unlesioned control ratio value. The amount of p75 ^{NTR}-positive neurons was increased after axotomy with and without application of TrkB-Fc; the increase is fully prevented by bumetanide. $n = 53$ slices/5800 neurons. $**p = 0.05$ (lesioned control)/0.028 (lesioned plus TrkB-Fc), one-way ANOVA and Bonferroni's *post hoc* analyses. ***e***, p75 ^{NTR} is not upregulated in the lesioned slices from NKCC1 knock-out mice. Data were obtained as in ***d***; $n = 37$ slices/3540 neurons. $**p = 0.02$, one-way ANOVA and Bonferroni's *post hoc* analyses. Error bars indicate SEM.

GACATCTCCTAGTTTGGACAGTG (Pgk1 RW) (Willems et al., 2006). Results were analyzed on Bio-Rad CFX Manager software and normalized to Pgk1.

Fluo-4[Ca^{2+}]$_i$ imaging
Neurons were loaded with Fluo-4 acetoxyl methyl (10 μM; Invitrogen) in extracellular standard solution containing the following (in mM): 124 NaCl, 3 KCl, 1.25 NaH$_2$PO$_4$, 1 MgSO$_4$, 26 NaHCO$_3$, 15 D-glucose, 2 CaCl$_2$; 5% CO$_2$/95% O$_2$. Slices were then laid on the glass bottom of a submerged-type chamber, and this was placed on a microscope stage and continuously perfused with standard solution gassed with 95% O$_2$/5% CO$_2$ at a rate of 2–3 ml/min. Fluo-4 fluorescence was visualized using a Leica TCS SP5 confocal system with a 20× objective lens (HCX APO L 20×/0.90 W; Leica) mounted on a DM5000 microscope (Leica). For excitation, a blue (OPSL 488 nm/270 mW) laser was used through a DD 488/561 beam splitter. Data were stored for off-line analysis by means of image-processing software LAS AF (Leica). Variations in [Ca^{2+}]$_i$ were observed as changes in intensities at 488 nm. Changes were monitored in the CA3 pyramidal neurons.

Statistical analysis
Statistical analysis was performed on PASW Statistic 18 software (SPSS). The normality of distribution was tested by Kolmogorov–Smirnov and Shapiro–Wilk tests (α level, 0.05). Comparison of mean values was performed by *t* test or one-way ANOVA followed by Bonferroni's *post hoc* analyses (α level, 0.05). Data are presented as mean ± SEM. Data are normalized to the values of unlesioned control slices, unless otherwise specified in the text. The average of raw values (percentage of cleaved caspase-3 or p75 ^{NTR}-positive neurons of total neuronal number) for the unlesioned control slices from all the experiments conducted during this current study were as follows: cleaved caspase-3 positive, 18 ± 2% (CA3)/21 ± 2% (CA1); p75 ^{NTR}-positive, 20 ± 1.5% (CA3)/ 20 ± 2% (CA1).

Results
Axotomized central neurons become dependent on endogenous BDNF
Survival of axotomized mature neurons is reduced upon withdrawal of endogenous BDNF, while intact mature neurons do not require BDNF for survival (Shulga et al., 2008). We used an *ex vivo* axotomy model in which an organotypic hippocampal slice is lesioned between CA3 and CA1 regions (Fig. 1*a*). We applied TrkB-Fc to withdraw endogenous BDNF. To assess the level of neuronal cell death, we performed double immunostaining for cleaved caspase-3 [a marker for cells committed to die through apoptosis (Logue and Martin, 2008)] and NeuN (a panneuronal marker) 24 h after the axotomy (Fig. 1*b*), and quantified the ratio of cleaved caspase-3-positive neurons to total NeuN-positive neuronal number. The lesion itself did not increase the number of apoptotic neurons (Fig. 1*c*). TrkB-Fc had no effect on the unlesioned slices; however, in the lesioned slices, it significantly increased the number of apoptotic neurons (Fig. 1*c*). Thus, decrease of endogenous BDNF after axotomy triggers the activation of apoptotic caspase-3. This indicates that hippocampal neurons become dependent on BDNF for survival upon trauma.

Emergence of posttraumatic BDNF requirement depends on p75 ^{NTR} function
We next asked what mediates the posttraumatic dependency on BDNF. p75 ^{NTR} is known to be upregulated after various kinds of injury (Chao, 2003), compete with Trk receptor signaling, and enhance the affinity and specificity of Trk receptors to their cognate ligands (Huang and Reichardt, 2001; Chao, 2003). To test whether p75 ^{NTR} is involved in the generation of dependency on BDNF after axotomy, we blocked p75 ^{NTR} with the function-blocking antibody recognizing the extracellular portion of p75 ^{NTR} (AB1554). This antibody completely prevented the significant increase in cleaved caspase-3-positive neuronal number upon TrkB-Fc application to the lesioned slices (Fig. 2*a,b*). The

effect was corroborated by the previously characterized Rex antibody known to inhibit $p75^{NTR}$ function (Weskamp and Reichardt, 1991) (Fig. 2b). Thus, when $p75^{NTR}$ was blocked, BDNF deprivation did not cause death of the axotomized neurons.

To further confirm the role of $p75^{NTR}$ in the apoptotic death of the neurons in our model, we turned to sortilin-deficient mice, as proneurotrophins elicit cell death through $p75^{NTR}$ only upon its association with sortilin coreceptor (Willnow et al., 2008). We applied TrkB-Fc to the lesioned organotypic slices prepared from sortilin$^{-/-}$ and wild-type mice of the same strain. In the wild-type slices, TrkB-Fc application again robustly increased the number of cleaved caspase-3-positive neurons, whereas in the sortilin$^{-/-}$ slices there was no effect of TrkB-Fc (Fig. 2c). In conclusion, the presence of functionally active $p75^{NTR}$ and sortilin is needed for the posttraumatic dependency of the neurons on BDNF.

It is known that $p75^{NTR}$ can promote apoptosis upon proneurotrophin binding (Chao, 2003); however, it is not clear to which extent neurotrophins are released in pro- form under physiological or pathological conditions (Matsumoto et al., 2008; Yang et al., 2009). To test whether endogenous proneurotrophins might activate signaling through $p75^{NTR}$, we aimed to decrease their concentration by application of plasmin, which cleaves extracellular proBDNF and proNGF to their mature forms (Lee et al., 2001). Plasmin significantly diminished the number of apoptotic neurons in TrkB-Fc-treated slices (Fig. 2d). Although plasmin has several targets, one possibility is that enhanced conversion of proneurotrophins to mature neurotrophins blocks the activation of the apoptotic cascade produced by the scavenging of endogenous BDNF. To test this idea, we applied blocking antibodies toward proNGF and proBDNF to lesioned slices treated with TrkB-Fc. Verification of the functional blocking effect of these antibodies was performed on basal forebrain primary cultures (Fig. 3). Here, we obtained similar results as previously shown by Volosin et al. (2006). Strikingly, the use of proNGF antibodies on hippocampal organotypic cultures completely abolished TrkB-Fc-induced death, while proBDNF antibodies had no effect (Fig. 2e). This result is in line with the previous data on the role of proNGF as an activating ligand for $p75^{NTR}$ in the in vivo axotomy model (Harrington et al., 2004). To verify that proNGF is present in the slices, we performed Western blot analyses with the same antibodies to proNGF that were used for functional blockage (Figs. 2f, 3). ProNGF expression was increased in the lesioned slices (119 ± 5% of unlesioned control). As expected, proNGF content was decreased by plasmin (Lee et al., 2001) (90 ± 5% of unlesioned
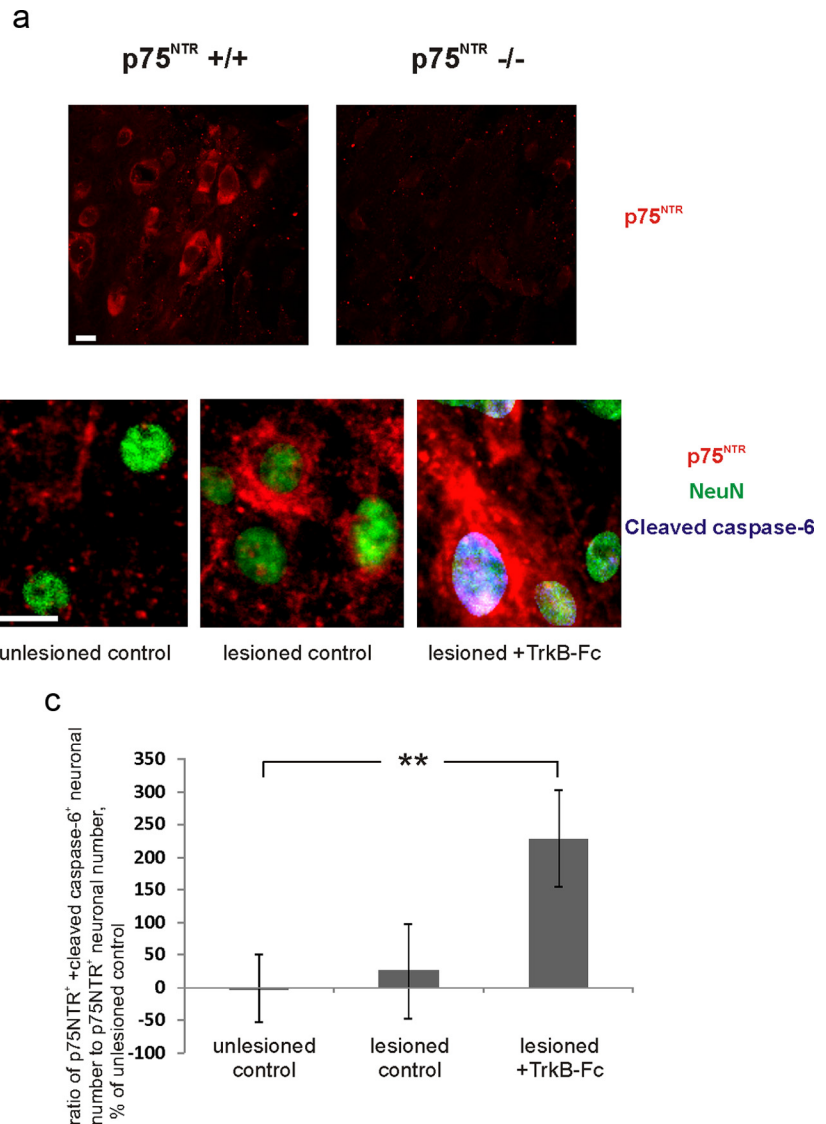
Figure 5. Increase in caspase-6/$p75^{NTR}$-positive neurons in the presence of Trkb-Fc after axotomy. **a**, Immunostainings of the basal forebrain showing the specificity of immunohistochemical staining with the antibody targeted against the extracellular portion of $p75^{NTR}$ AB1554 in wild type but not in $p75^{NTR-/-}$ animals. Scale bar, 10 μm. **b**, Fragments of representative confocal images from unlesioned, lesioned, and lesioned TrkB-Fc-treated hippocampal organotypic slices stained immunohistochemically for NeuN (green), $p75^{NTR}$ (red), and cleaved caspase-6 (blue). Scale bar, 10 μm. **c**, Ratio of $p75^{NTR}$ plus cleaved caspase-6-positive neuronal number to $p75^{NTR}$-positive neuronal number, obtained by stereological counting in the CA3 region, percentage of unlesioned control ratio value. Cleaved caspase-6 channel was masked with NeuN channel (see Materials and Methods). $n = 12$ slices/87 neurons; **$p = 0.05$, two-tailed t test versus unlesioned control. Error bars indicate SEM.

control; Fig. 2f), which is in line with the antiapoptotic effect of this agent (Fig. 2d).

In conclusion, proNGF as well as $p75^{NTR}$ and sortilin are essential for the induction of posttraumatic dependency on BDNF trophic support, since elimination of any of these factors renders injured neurons nonresponsive to endogenous BDNF withdrawal.

Specific inhibition of NKCC1 with bumetanide prevents BDNF withdrawal-induced death and posttraumatic upregulation of $p75^{NTR}$

Postaxotomy induction of dependency on BDNF can be prevented by the NKCC1-specific (Blaesse et al., 2009) inhibitor bumetanide, which prevents posttraumatic GABA-induced intracellular Ca^{2+} increase (Shulga et al., 2008). The mechanism
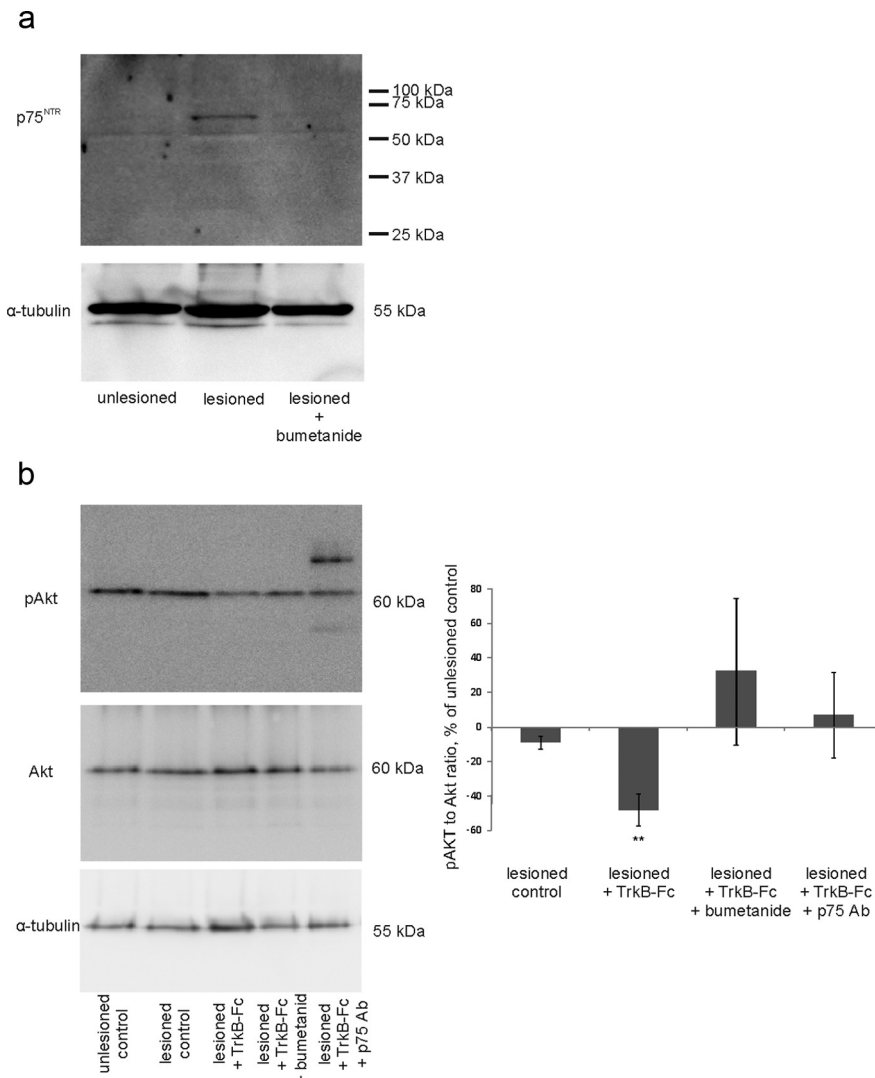
a

b

Figure 6. *a*, Western blot analyses with antibody 9651 (Huber and Chao, 1995) from whole-slice homogenates show postaxotomy upregulation of p75^{NTR}, which is prevented by bumetanide. p75^{NTR} is normalized to α-tubulin. $n = 3$ experiments/36 slices; **$p = 0.028$, one-way ANOVA and Bonferroni's *post hoc* analyses. *b*, pAkt/Akt ratio is decreased in lesioned TrkB-Fc-treated slices, whereas treatment with antibody to p75^{NTR} or bumetanide returns it to the level of the unlesioned control. Phospho-Akt is normalized to pan-Akt; $n = 3$ experiments/60 slices; **$p = 0.007$ by two-tailed *t* test versus unlesioned control. Additional bands in lesioned plus p75Ab-treated sample result from the staining of rabbit-anti p75Ab used for function blocking with secondary anti-rabbit antibody. Error bars indicate SEM.

behind nonresponsiveness to BDNF withdrawal in bumetanide-treated neurons is an open question. Here, we tested whether neuronal death is prevented by bumetanide in BDNF-deprived injured neurons. As expected, bumetanide application prevented the increase in the number of apoptotic neurons in TrkB-Fc-treated lesioned slices (Fig. 4*a*).

Since interfering with p75^{NTR} function and applying bumetanide had the same effect, we next asked whether bumetanide affects p75^{NTR} expression. We measured p75^{NTR} mRNA expression from the whole slice. There was no significant difference in p75^{NTR} mRNA levels at 1–2 h (Fig. 4*b*), but 6 h after axotomy p75^{NTR} mRNA levels were significantly increased (Fig. 4*b*; 136 ± 1%). Strikingly, this increase was not present in the bumetanide-treated slices (Fig. 4*b*; 85 ± 1%).

To monitor the neuronal, region-specific expression of p75^{NTR}, we performed immunohistochemical stainings with an antibody targeted against the extracellular portion of p75^{NTR},

which inhibits p75^{NTR} function (AB1554; see above). The specificity of this antibody has been previously verified by the lack of immunostaining in basal forebrain neurons of p75$^{-/-}$ animals (Gehler et al., 2004; Dhanoa et al., 2006) (Fig. 5*a*). We made high-magnification confocal image stacks and counted the ratio of p75^{NTR}-positive neurons to total neuronal number from 3D reconstruction images (Fig. 4*c*) (see Materials and Methods). There was a significant increase in the number of p75^{NTR}-positive neurons after the lesion both in the absence and in the presence of TrkB-Fc (Fig. 4*d*). However, there was a significant increase in apoptotic neuronal number [as indicated by cleaved caspase-6 (Wang et al., 2001; Troy et al., 2002) colocalization with neuronal nuclei] in the pool of p75^{NTR}-positive neurons only in the presence of TrkB-Fc (Fig. 5*b,c*).

Strikingly, bumetanide treatment completely abolished the increase in the number of p75^{NTR}-positive neurons (Fig. 4*d*). Also, genetic deletion of NKCC1 fully prevented posttraumatic upregulation of p75^{NTR} (Fig. 4*e*). Bumetanide did not have a significant effect on p75^{NTR} expression in the unlesioned slices (Fig. 4*d*).

We also measured p75^{NTR} expression by Western blot analyses from whole slice homogenates with an antibody to the extracellular portion of p75^{NTR} (Huber and Chao, 1995) (9651) and observed postaxotomy upregulation of p75^{NTR} (136 ± 2% of unlesioned control), which was prevented by bumetanide (lesioned plus bumetanide: 102 ± 11% of unlesioned control; Fig. 6*a*). Thus, inhibition of NKCC1-dependent chloride accumulation blocked the lesion-induced increase in p75^{NTR} expression and death produced by the reduction of endogenous BDNF.

Increased cell death is reflected in the decrease of survival signaling. p75^{NTR} signaling is known to interfere with PI-3 kinase survival pathway downstream Trk receptors in cell lines (Huang and Reichardt, 2001). To investigate whether interfering with p75^{NTR} function or applying bumetanide enhances survival signaling in neurons, we measured phosphorylation of Akt (also known as PKB), a major survival-promoting kinase in the neurons (Huang and Reichardt, 2001), from the whole-slice homogenates. Akt phosphorylation was significantly reduced in TrkB-Fc-treated lesioned slices; treatment with either blocking antibody to p75^{NTR} or bumetanide prevented this decrease (Fig. 6*b*). There was no significant change in Akt expression (lesioned control: 91 ± 4%; lesioned plus TrkB-Fc: 106 ± 12%; lesioned plus TrkB-Fc plus bumetanide: 113 ± 26%; lesioned plus TrkB-Fc plus p75^{NTR} Ab: 135 ± 27%; $n = 60$ slices; pan-Akt normalized to α-tubulin; here and elsewhere in the text, the data are presented as percentage of unlesioned control slices ratio value, unless otherwise specified). ProNGF has been shown to prevent the ability of BDNF to induce phosphorylation of Akt

(Volosin et al., 2006) through phosphatase PTEN (phosphatase and tensin homolog deleted on chromosome 10) (Song et al., 2010). Thus, it is possible that, due to the low concentration of TrkB-Fc used in these experiments, the level of endogenous BDNF, which is lowered dramatically by TrkB-Fc, becomes nonetheless sufficient to maintain the phosphorylation of Akt in the absence of the opposing signaling of proNGF through $p75^{NTR}$.

Posttraumatic depolarizing shift in $GABA_A$-mediated responses occurs shortly after injury

To determine whether a change in $GABA_A$-mediated responses is established at an early stage after injury, we monitored $[Ca^{2+}]_i$ evoked by the $GABA_A$-specific agonist muscimol in the CA3 region of organotypic cultures 3–4 h after injury (Fig. 7). A larger proportion of monitored neurons responded with $[Ca^{2+}]_i$ increase to muscimol in injured slices than in uninjured controls (100 μM; unlesioned control: 3 ± 1% of total recorded neurons; n = 172 pyramidal cells; lesioned: 61 ± 9% of total recorded neurons; n = 269 pyramidal cells). This effect was completely inhibited by blocking intracellular chloride accumulation with the NKCC1 inhibitor bumetanide (10 μM; lesioned: 1 ± 0.3% of total recorded neurons; n = 244 pyramidal cells). All monitored cells responded to glutamate (100 μM). These results are consistent with our previous finding (Shulga et al., 2008). The presence of depolarizing $GABA_A$-mediated responses as soon as 3 h after axotomy reinforces the causal relationship between this event and the upregulation of $p75^{NTR}$.

We found no changes in NKCC1 (111 ± 24% of unlesioned control; n = 3 experiments/24 slices; p > 0.1 by two-tailed t test) and in KCC2 protein expression (126 ± 17% of unlesioned control; n = 3 experiments/24 slices; p > 0.1 by two-tailed t test) 4 h after axotomy by Western blot analyses (Fig. 8a,b). KCC2 and NKCC1 are regulated also at the functional level (e.g., the proportion of membrane-bound transporters and/or the change in the intrinsic rate of ion transport can be affected). Recent evidence shows that phosphorylation at tyrosine residues of the KCC2 protein decreases membrane stability, which results in reduced chloride extrusion efficiency (Lee et al., 2010). Intriguingly, we observed a significant increase in KCC2 phosphorylation 4 h after axotomy (Fig. 8c,d). Thus, the present data indicate that an early posttraumatic reduction in functional KCC2 expression could be crucially involved in the changes in $GABA_A$-mediated responses.

Posttraumatic upregulation of $p75^{NTR}$ depends on membrane depolarization and activation of voltage-gated Ca^{2+} channels

The results above show that, after trauma, bumetanide can block $GABA_A$ agonist-induced increase in $[Ca^{2+}]_i$ (Shulga et al., 2008), which is mediated by GABA-induced depolarization and consequent opening of voltage-gated Ca^{2+} channels (Blaesse et al., 2009). We tested whether intracellular Ca^{2+} and activation of voltage-gated Ca^{2+} channels are important for the posttraumatic $p75^{NTR}$ upregulation. We chelated intracellular Ca^{2+} by application of BAPTA-AM (100 μM). This treatment completely abol-
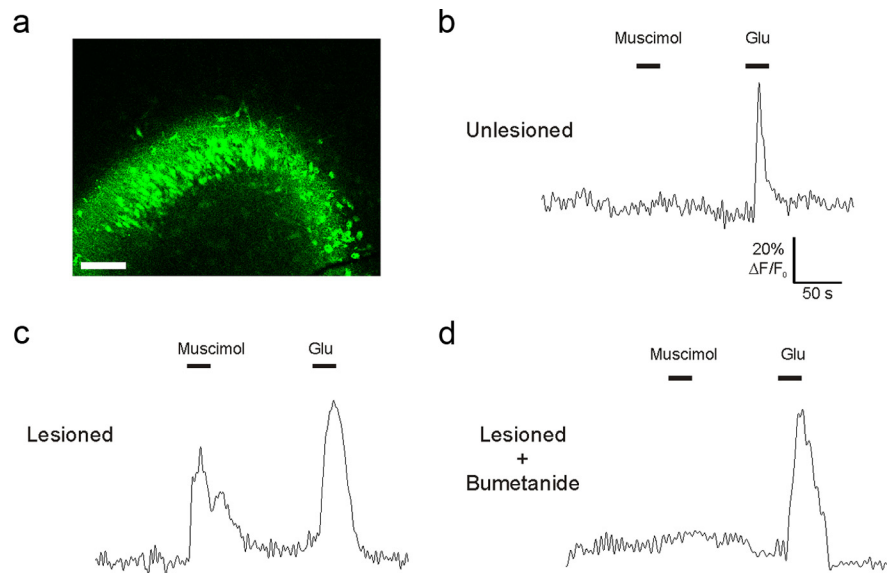
Figure 7. $GABA_A$-mediated responses become depolarizing shortly after axotomy. $[Ca^{2+}]_i$ was monitored with Fluo-4 in hippocampal organotypic cultures. **a**, Loading of Fluo-4 in the CA3 of an axotomized organotypic culture. Scale bar, 250 μm. **b–d**, Representative recordings from unlesioned and lesioned slices. Muscimol could evoke $[Ca^{2+}]_i$ increase in lesioned (**c**) but not in unlesioned (**b**) slices already 3 h after axotomy. Application of NKCC1 inhibitor bumetanide to the perfusion was able to block this effect (**d**). Glutamate application was used to ensure the viability of the slice (**b–d**). n = 3–4 slices per experimental group.

ished the posttraumatic increase in the number of $p75^{NTR}$-positive neurons (Fig. 9a). We next blocked voltage-gated Ca^{2+} channels with Ni^{2+}/Cd^{2+} (100 μM), which also completely abolished posttraumatic increase in $p75^{NTR}$ (Fig. 9a). Inhibition of L-type voltage-gated Ca^{2+} channels with nimodipine (20 μM) gave a similar outcome (lesioned: 356 ± 102%; lesioned plus nimodipine: 94 ± 34% of unlesioned control; n = 21 slices; p = 0.05 by one-way ANOVA and Bonferroni's *post hoc* analyses). These results pinpoint L-type Ca^{2+} channel activation as an important step in the mechanism of trauma-induced $p75^{NTR}$ upregulation.

GABA-mediated depolarization is able to upregulate $p75^{NTR}$ in the absence of action potential firing

$GABA_A$-mediated depolarization in axotomized neurons could increase the probability of action potential firing. This in turn could increase Ca^{2+}-regulated vesicular release of GABA (Farrant and Kaila, 2007). Consequently, the effect of bumetanide on $p75^{NTR}$ could be mediated not only through direct prevention of depolarization-induced activation of voltage-gated Ca^{2+} channels but also through a reduction in excitability, neuronal activity, and GABA release. To discriminate between these possibilities, we looked at $p75^{NTR}$ expression after application of voltage-gated Na^+ channel blocker TTX (2 μM), $GABA_A$ agonist muscimol (50 μM), and voltage-gated K^+ channel blocker 4-AP (100 μM). To test whether $GABA_A$-mediated depolarization can upregulate $p75^{NTR}$ in the absence of action potential firing, we applied TTX to the lesioned slices. Although TTX reduced the amount of $p75^{NTR}$-positive neurons to a level that did not differ significantly from the unlesioned control values, it did not, unlike bumetanide, fully block the posttraumatic $p75^{NTR}$ upregulation (Fig. 9b). Increasing the concentration of TTX from 2 to 10 μM did not result in the increase of TTX efficiency (lesioned control, 216 ± 8%; lesioned plus 10 μM TTX, 157 ± 50%; n = 12 slices/1490 neurons). Thus, reduction in activity does not fully account for the effect of bumetanide. TTX could reduce Ca^{2+}-regulated release of GABA (Farrant and Kaila, 2007); to address the ques-
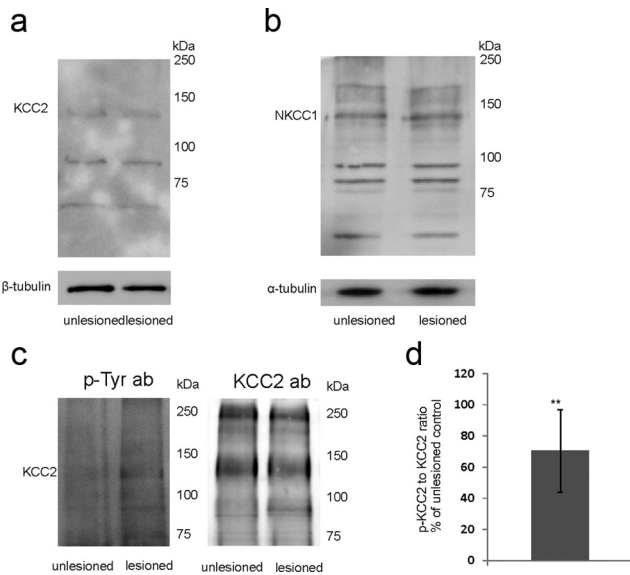
Figure 8. Western blot analyses from the whole slices 4 h after axotomy. No change in protein expression of KCC2 (***a***) or NKCC1 (***b***) was observed. ***c***, Representative Western blot from lysates immunoprecipitated with anti-KCC2 antibody, stained for phosphotyrosine and KCC2. ***d***, Ratio of tyrosine-phosphorylated KCC2 to total KCC2, percentage of unlesioned control. $n = 3$ experiments/96 slices; **$p = 0.05$, two-tailed t test. Error bars indicate SEM.

tion whether this could explain the TTX-induced reduction in the amount of $p75^{NTR}$-positive neurons, we added muscimol to compensate for this effect. In the lesioned TTX-treated slices, muscimol increased the number of $p75^{NTR}$-positive neurons to the level of the lesioned control values, and the effect of muscimol could be blocked with bumetanide. On the contrary, addition of the GABA$_A$ antagonist bicuculline (20 μM) in the presence of TTX completely abolished lesioned-induced increase in $p75^{NTR}$ expression, further verifying the idea that GABA$_A$ receptors are crucial for posttraumatic $p75^{NTR}$ upregulation, and that incomplete blockade of this upregulation by TTX results from the incomplete blockade of GABA release (TTX does not block the spontaneous release of GABA) (Fig. 9b). Thus, GABA$_A$-mediated depolarization upregulates $p75^{NTR}$ in the absence of neuronal activity. To enhance neuronal activity in the absence of GABA-mediated depolarization, we applied 4-AP in the presence of bumetanide. This did not result in a significant increase in the amount of $p75^{NTR}$-positive neurons (Fig. 9b).

We also tested whether $p75^{NTR}$ upregulation can be induced in nonaxotomized slices by conditions mimicking posttraumatic GABA-mediated depolarization in the absence of enhanced activity. Slices were subjected to prolonged exposure (24 h) to high potassium (10 mM) in the presence of TTX. A modest increase in extracellular K^+ reverses KCC2-mediated K^+–Cl^+ transport leading to accumulation of intracellular chloride (Farrant and Kaila, 2007). TTX was added 30 min and 15 min before potassium chloride (KCl) on top of the slice and after that added to the medium together with KCl. The treatment resulted in a significant increase in the number of $p75^{NTR}$-positive neurons, the magnitude of the effect being comparable with the effect of the lesion. The effect of KCl could be blocked by Ni^{2+}/Cd^{2+}, suggesting that membrane depolarization upregulates $p75^{NTR}$ through opening of voltage-gated Ca^{2+} channels (Fig. 9c).
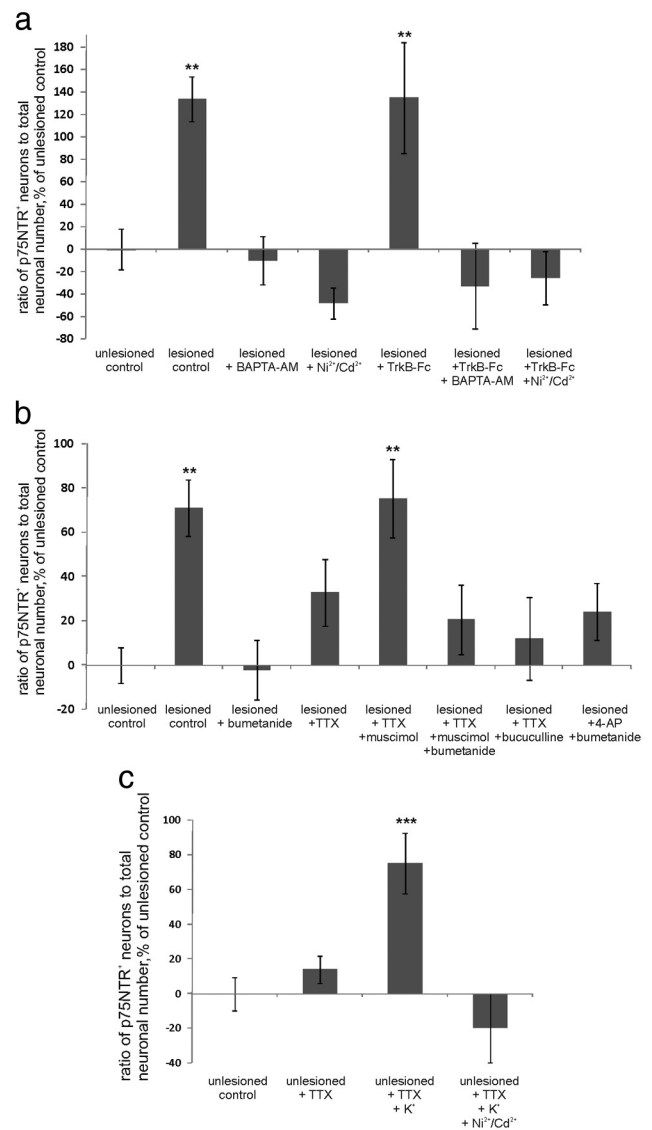

Figure 9. $p75^{NTR}$ is upregulated by a mechanism requiring membrane depolarization and opening of voltage-gated Ca^{2+}-channels. ***a–c***, Data obtained as in Figure 4d. ***a***, Application of BAPTA-AM (intracellular calcium chelator) as well as of Ni^{2+}/Cd^{2+} (blocker of voltage-gated calcium channels) prevented posttraumatic upregulation of $p75^{NTR}$. $n = 29$ slices/3290 neurons; **$p = 0.041$ (lesioned control)/0.039 (lesioned plus TrkB-Fc), one-way ANOVA and Bonferroni's *post hoc* analyses. ***b***, Application of voltage-gated Na^+ channel blocker TTX partly reduced the upregulation of $p75^{NTR}$. Adding GABA$_A$ agonist muscimol in the presence of TTX restored the level of $p75^{NTR}$ to the level of lesioned control; the effect of muscimol could be abolished by bumetanide. Adding GABA$_A$ antagonist bicuculline in the presence of TTX completely abolished the increase in $p75^{NTR}$. Applying K^+ channel blocker 4-AP in the presence of bumetanide did not result in the significant increase in the number of $p75^{NTR}$-positive neurons; $n = 128$ slices/13,600 neurons; **$p = 0.037$ (lesioned control)/0.019 (lesioned plus TTX plus muscimol), one-way ANOVA and Bonferroni's *post hoc* analyses. ***c***, Application of KCl and TTX to induce membrane depolarization in the absence of action potential firing upregulated $p75^{NTR}$ in nonaxotomized slices; the effect could be blocked by Ni^{2+}/Cd^{2+}; $n = 48$ slices/5490 neurons; ***$p = 0.001$, one-way ANOVA and Bonferroni's *post hoc* analyses. Error bars indicate SEM.

Posttraumatic $[Ca^{2+}]_i$ increase activates Rho kinase to upregulate $p75^{NTR}$

After spinal cord injury, there is an increase in the activation of the small GTPase Rho. Interestingly, Rho antagonist halts the posttraumatic increase in $p75^{NTR}$ (Dubreuil et al., 2003). In nonneuronal cells, the activation of Rho and its downstream effector Rho kinase (ROCK) is induced by depolarization-induced activation of voltage-gated Ca^{2+} channels (Sakurada et al., 2003; Liu

et al., 2005); RhoA is also activated down-stream the complex of $p75^{NTR}$ with NgR and LINGO1 receptors in neurons (McKerracher and Higuchi, 2006). To test whether ROCK has a role in the posttraumatic $p75^{NTR}$ upregulation in the present injury model, we applied the ROCK inhibitor Y-27632. Strikingly, this treatment completely abolished the rise in the amount of $p75^{NTR}$-positive neurons after axotomy both in the presence and in the absence of TrkB-Fc (Fig. 10a). ROCK inhibitor also prevented the KCl-induced upregulation of $p75^{NTR}$ (mediated by opening of voltage-gated Ca^{2+} channels; see above) in intact CA3 neurons (Fig. 10a).

To elucidate whether ROCK is acting downstream or upstream of the posttraumatic $[Ca^{2+}]_i$ increase, we monitored $[Ca^{2+}]_i$ at 3–4 h after axotomy (when $GABA_A$ agonist already is able to induce $[Ca^{2+}]_i$ increase; see above), in the presence of Y-27632, which was applied at the same time with the lesion. We observed no reduction in the ability of muscimol to induce $[Ca^{2+}]_i$ increase after axotomy by Y-27632 ($65.3 \pm 7.2\%$ of total recorded neurons; $n = 256$ pyramidal cells) compared with lesioned control slices (see above). Thus, we concluded that ROCK is acting downstream of the $[Ca^{2+}]_i$ increase.

To further verify this idea, as well as to test whether ROCK can be activated by Ca^{2+} not only in non-neuronal cells (Sakurada et al., 2003; Liu et al., 2005) but also in neural tissue, we used phospho-cofilin as a marker of ROCK activation (Maekawa et al., 1999). We normalized total p-cofilin immunostaining intensity measured from the middle of the CA3 region to total number of cells in the same region (Fig. 10b,c). We observed a significant increase in total p-cofilin staining intensity after axotomy. This increase was not present upon application of Y-27632, which verifies that axotomy induces an increase in ROCK activation. Notably, posttraumatic increase in cofilin phosphorylation was also prevented by bumetanide and Ni^{2+}/Cd^{2+}, indicating the crucial role of posttraumatic GABA-mediated depolarization and $[Ca^{2+}]_i$ increase through voltage-gated Ca^{2+} channels in the activation of ROCK. Thus, $GABA_A$-induced $[Ca^{2+}]_i$ increase leads to upregulation of $p75^{NTR}$ through the activation of Rho kinase.

Denervation and axotomy-induced cell death share similar mechanisms

While in the *ex vivo* lesion model the CA3 region is axotomized, the CA1 region is subjected to denervation. To investigate the cell death mechanism in the denervated neurons, we quantified the CA1 region of slices from the key experiments described above. The data are summarized in Figure 11. Interestingly, in the CA1
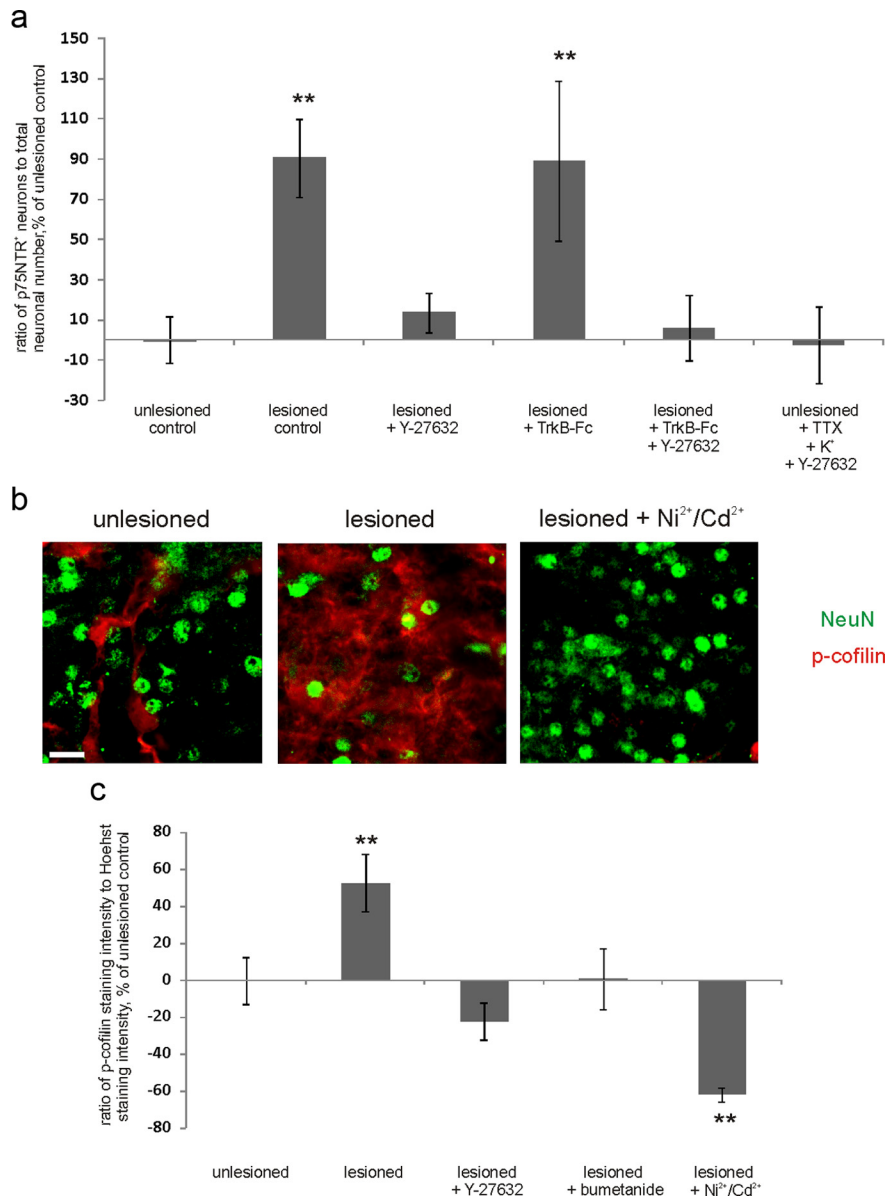

Figure 10. Posttraumatic $[Ca^{2+}]_i$ increase induces ROCK activation to increase $p75^{NTR}$ expression. ***a***, ROCK inhibitor Y-27632 completely abolished posttraumatic $p75^{NTR}$ upregulation in the presence and in the absence of TrkB-Fc, as well as KCl-induced upregulation of $p75^{NTR}$; $n = 58$ slices/5750 neurons; **$p = 0.006$ (lesioned control) and 0.024 (lesioned plus TrkB-Fc), one-way ANOVA and Bonferroni's *post hoc* analyses. ***b***, Fragments of representative confocal images from the CA3 region of unlesioned, lesioned, and lesioned Ni^{2+}/Cd^{2+}-treated slices stained immunohistochemically for NeuN (green) and p-cofilin (red). Scale bar, 10 μm. ***c***, Quantification of p-cofilin staining intensity measured from the middle of the CA3 region, normalized to Hoechst staining intensity. P-cofilin staining intensity is induced by lesion, but not in the presence of Y-27632, bumetanide, or Ni^{2+}/Cd^{2+}; $n = 46$ slices; **$p = 0.024$ (lesioned control)/0.003 (lesioned plus Ni^{2+}/Cd^{2+}), one-way ANOVA and Bonferroni's *post hoc* analyses. Error bars indicate SEM.

region there was a significant increase in the number of $p75^{NTR}$-positive neurons after axotomy only in the presence of TrkB-Fc (Fig. 11e); there was also no activation of ROCK in the CA1 region of the lesioned slices in the absence of TrkB-Fc (as indicated by p-cofilin staining intensity normalized to Hoechst staining intensity; $89 \pm 23\%$ of unlesioned control; $n = 16$ slices).

Posttraumatic upregulation of $p75^{NTR}$ and cell death induction is blocked by bumetanide *in vivo*

Finally, we tested whether the proposed mechanism of $p75^{NTR}$ upregulation is relevant *in vivo*. We used a model in which spinal motoneurons are axotomized at the level of the ventral root (Ris-
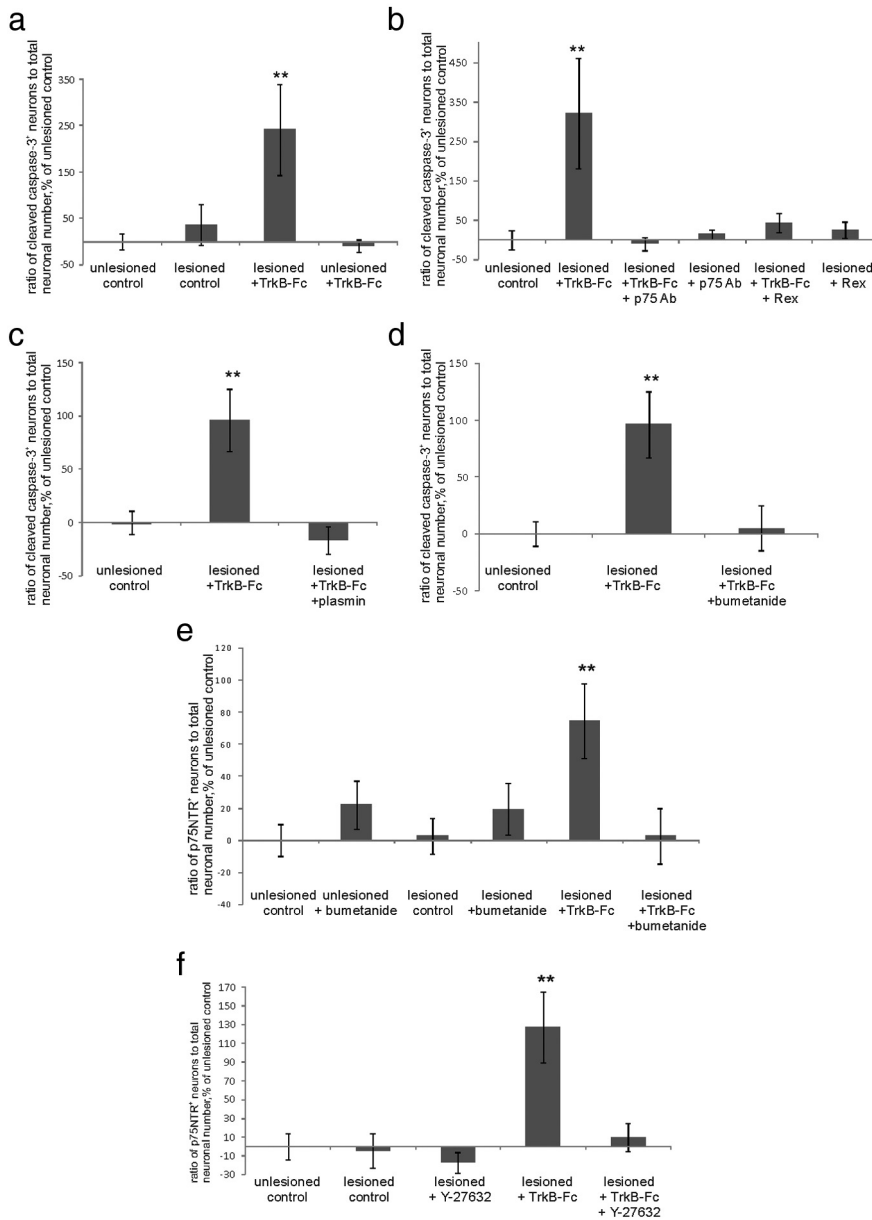
Figure 11. Cell death in denervated neurons in the CA1 region is induced by similar mechanism as in the axotomized neurons. ***a–d***, Ratio of cleaved caspase-3-positive neuronal number to total neuronal number obtained by blind stereological counting in the CA1 region, percentage of unlesioned control ratio value. ***a***, TrkB-Fc induces a significant increase in apoptotic neuronal number in the lesioned, but not unlesioned, slices at 1 d after the injury; $n = 43$ slices/4800 neurons; $**p = 0.013$, one-way ANOVA and Bonferroni's *post hoc* analyses. ***b***, Treatment with function-blocking antibodies to $p75^{NTR}$ (Fig. 2b) abolished the increase in the number of apoptotic neurons promoted by TrkB-Fc; $n = 46$ slices/4890 neurons; $**p = 0.002$, one-way ANOVA and Bonferroni's *post hoc* analyses. ***c***, Treatment with plasmin abolished the TrkB-Fc-induced increase in the number of apoptotic neurons; $n = 33$ slices/3990 neurons; $**p = 0.004$, one-way ANOVA and Bonferroni's *post hoc* analyses. ***d***, Bumetanide abolishes the death induction in neurons deprived of BDNF; $n = 33$ slices/3750 neurons; $**p = 0.007$, one-way ANOVA and Bonferroni's *post hoc* analyses. ***e,f***, Ratio of $p75^{NTR}$-positive neuronal number to total neuronal number, obtained by blind stereological counting in the CA1 region, percentage of unlesioned control ratio value. ***e***, The amount of $p75^{NTR}$-positive neurons was increased after axotomy only in the presence of TrkB-Fc; the increase was fully blocked by bumetanide; $n = 56$ slices/7800 neurons; $**p = 0.032$, one-way ANOVA and Bonferroni's *post hoc* analyses. ***f***, ROCK inhibitor Y-27632 completely abolished posttraumatic $p75^{NTR}$ upregulation in the presence of TrkB-Fc; $n = 58$ slices/5840 neurons; $**p = 0.002$ (lesioned plus TrkB-Fc), one-way ANOVA and Bonferroni's *post hoc* analyses. Error bars indicate SEM.

ling et al., 1992) (Fig. 12a) (see also Materials and Methods). Strikingly, this treatment resulted in the profound upregulation of $p75^{NTR}$ in injured motoneurons, which was blocked by intraperitoneal administration of bumetanide (30 mg/kg). Results of the quantification of $p75^{NTR}$-positive neurons normalized to to-

tal neuronal number are presented in Figure 12, *b* and *c*. Results without normalization are as follows: lesioned control, $928 \pm 141\%$; lesioned plus bumetanide, $222 \pm 41\%$ of unlesioned control (quantified as in Fig. 12c; $p = 0.002$ by ANOVA and Bonferroni's *post hoc* analysis). We also observed a significant increase in the amount of cleaved caspase-3-positive neurons in the spinal cords of lesioned control rats, which was blocked by bumetanide administration (Fig. 12e,f). We have also quantified the number of NeuN-positive motoneurons as follows (see Materials and Methods): unlesioned, 108 ± 6 neurons; lesioned, 28 ± 7 neurons; lesioned plus bumetanide, 67 ± 11 neurons in 4 sections ($p = 0.005$ by one-way ANOVA). KCC2 immunostaining intensity was significantly reduced in injured neurons (Nabekura et al., 2002) ($80 \pm 3\%$ of unlesioned control; Fig. 12d; identified by the same criteria as $p75^{NTR}$-positive neurons) (see Materials and Methods). Thus, blockade of NKCC1 prevents posttraumatic upregulation of $p75^{NTR}$ and cell death *in vivo*.

Discussion

$p75^{NTR}$ is upregulated under various pathological conditions, including seizures, ischemia, neurodegeneration, osmotic swelling, and mechanical damage, with levels of reexpression being comparable with levels seen during early development (Dechant and Barde, 2002; Chao, 2003; Peterson and Bogenmann, 2003). These insults are also followed by functional downregulation of KCC2 and the consequent accumulation of intracellular chloride through NKCC1 and depolarizing responses to GABA (Blaesse et al., 2009). We show here *ex vivo* and in a clinically relevant *in vivo* model (Risling et al., 1992; Carlstedt, 2008) that the axotomy-induced upregulation of $p75^{NTR}$ can be prevented by blocking $GABA_A$-mediated depolarization or subsequent activation of voltage-gated Ca^{2+} channels. Therefore, our results strongly indicate that postaxotomy reexpression of $p75^{NTR}$ is induced by the shift in the polarity of GABA-mediated responses. Our data open the theoretical possibility that similar mechanism regulates $p75^{NTR}$ also in other pathological conditions such as seizures and neurodegeneration.

After trauma, $GABA_A$-mediated $[Ca^{2+}]_i$ increase induces the dependency on BDNF trophic support (Shulga et al., 2008). Endogenous BDNF is not required for the survival of intact adult neurons (Giehl et al., 2001; Li et al., 2008; Shulga et al., 2008; Rauskolb et al., 2010). However, there is a positive therapeutic effect of BDNF

in injured adult neurons (Klöcker et al., 2000; Schäbitz et al., 2000; Shulga et al., 2008, 2009). The exact reason for this shift is not known. The results in this study indicate that upregulation of $p75^{NTR}$ is responsible for setting the dependency on BDNF for survival.

In the *in vivo* axotomy model in which corticospinal neurons are lesioned, neuronal death occurs without BDNF scavenger (Giehl et al., 2001; Harrington et al., 2004; Shulga et al., 2008). However, scavenging endogenous BDNF in these neurons results in further neuronal loss (Shulga et al., 2008), whereas application of exogenous BDNF completely prevents axotomy-induced neuronal loss and atrophy (Giehl and Tetzlaff, 1996). Thus, appearance of postaxotomy dependency on BDNF trophic support for survival, as well as shortage of endogenous BDNF and the resultant neuronal death, are phenomena that occur *in vivo*. Accordingly, in the corticospinal neuron lesion model (Giehl et al., 2001; Harrington et al., 2004; Shulga et al., 2008) and in ventral root axotomy model used in this work, neuronal death occurs most probably due to lack of endogenous BDNF *in vivo*. Blocking $p75^{NTR}$ with Rex antibody (Giehl et al., 2001) or using $p75^{-/-}$ (Harrington et al., 2004) or sortilin$^{-/-}$ animals (Jansen et al., 2007) prevents axotomy-induced neuronal death in corticospinal neurons. In the organotypic culture axotomy model, death of axotomized CA3 region neurons occurs only in the presence of TrkB-Fc (Shulga et al., 2008), most probably because endogenous BDNF that is highly expressed in the DG and CA3 regions (Conner et al., 1997) triggers survival signaling that overwhelms the death signaling from $p75^{NTR}$. Thus, the *ex vivo* model used in this work allows monitoring the requirement for namely endogenous BDNF.

To elucidate the mechanism regulating $p75^{NTR}$ levels in more detail, we applied the voltage-gated Na^+ channel blocker TTX and the voltage-gated K^+ channel blocker 4-AP and observed that $GABA_A$-mediated depolarization was able to increase the $p75^{NTR}$ expression in the absence of action potential firing, whereas enhancement of activity in the absence of $GABA_A$-mediated depolarization did not have an effect on $p75^{NTR}$ levels. Interestingly, the inhibitor of ROCK, the downstream effector of small GTPase Rho, was as effective as bumetanide in preventing the posttraumatic upregulation of $p75^{NTR}$. It has been shown that inhibiting Rho prevents upregulation of $p75^{NTR}$ after spinal cord injury (Dubreuil et al., 2003). We now show that the activation of one of its effectors ROCK is the mechanism coupling $GABA_A$-mediated $[Ca^{2+}]_i$ increase and the posttraumatic $p75^{NTR}$ up-
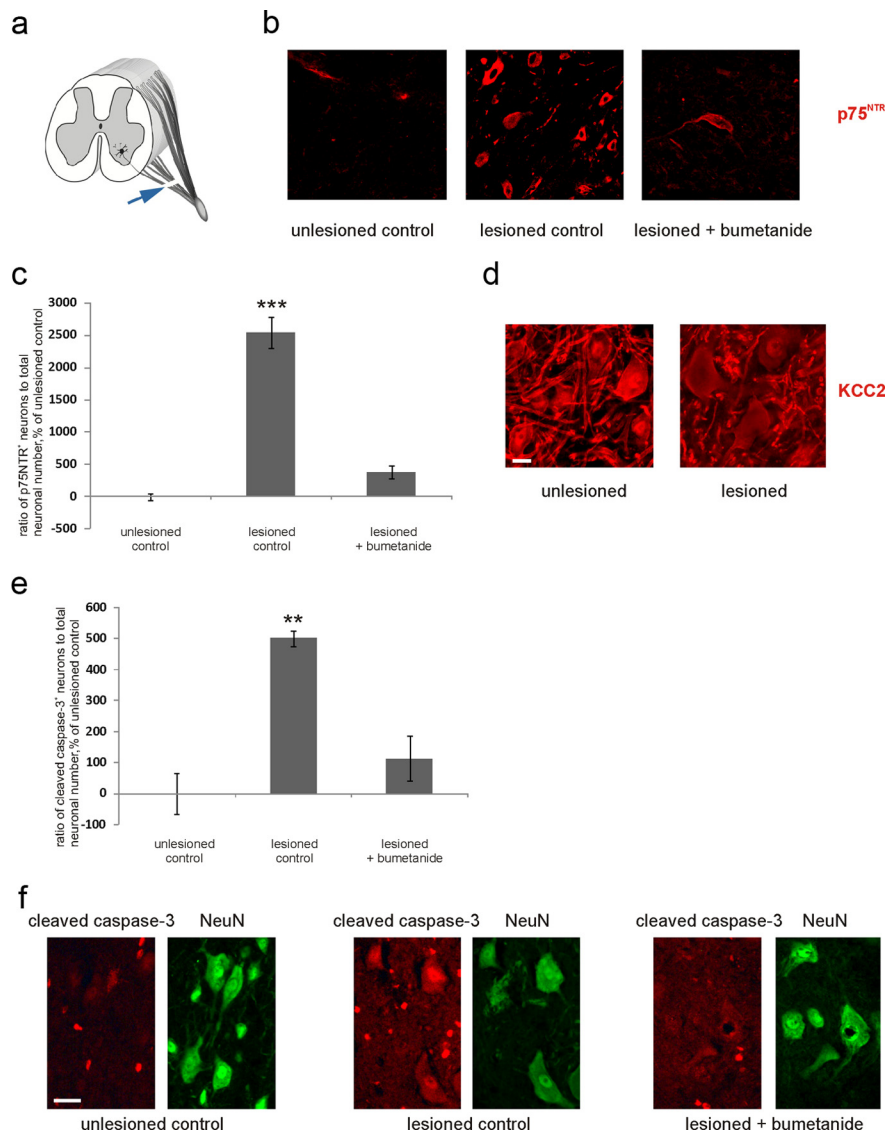
Figure 12. Bumetanide prevents upregulation of $p75^{NTR}$ and cell death induction after *in vivo* ventral root axotomy. ***a***, Schematic representation of the injury. Axotomy of spinal motoneurons was performed at the ventral root between the spinal cord and the junction with the dorsal root (for details, see Materials and Methods). Arrow, Lesion site. ***b***, Representative images from the sections of the spinal cords of unlesioned, lesioned (by ventral root axotomy), and lesioned bumetanide-treated rats at the level of the injury stained immunohistochemically for $p75^{NTR}$. Scale bar, 30 μm. ***c***, Quantification of $p75^{NTR}$-positive neurons from the similar sections as in ***b***. Total amount of $p75^{NTR}$-positive neurons from four sections of the spinal cord and total amount of neurons (NeuN-defined) from four sections consecutive to each $p75^{NTR}$-stained section was counted by blind stereological counting from ventral horns (for selection criteria, see Materials and Methods) and the $p75^{NTR}$/NeuN ratio for each animal quantified. Data are presented as percentage of unlesioned control ratio. $n = 3$ unlesioned, 2 lesioned, 3 lesioned bumetanide-treated rats. ***p < 0.001, one-way ANOVA and Bonferroni's *post hoc* analyses. ***d***, Representative images of sections as in ***b*** stained immunohistochemically for KCC2. Scale bar, 15 μm. KCC2 immunostaining intensity, measured from images similar as in ***d***, is reduced in neurons in the ventral horn of the lesioned animals. $n = 18$ sections/5 animals; **p = 0.004, one-way ANOVA and Bonferroni's *post hoc* analyses. ***e***, Quantification of cleaved caspase-3-positive neurons performed as in ***c*** from similar sections as in ***f***. NeuN was detected from the same sections as cleaved caspase-3; $n = 3$ unlesioned, 2 lesioned, 3 lesioned bumetanide-treated rats; **p = 0.012, one-way ANOVA and Bonferroni's *post hoc* analyses. ***f***, Representative images from the sections of the spinal cords of unlesioned, lesioned, and lesioned bumetanide-treated rats at the level of the injury stained immunohistochemically for cleaved caspase-3 and NeuN. Scale bar, 30 μm. Error bars indicate SEM.

regulation. In non-neuronal cells, Rho–ROCK pathway has been shown to be activated through membrane depolarization-induced opening of voltage-gated Ca^{2+} channels (Sakurada et al., 2003; Liu et al., 2005), and here we show that ROCK can be activated by the same mechanism also in neural tissue.

The proposed mechanism of the emergence of neuronal dependency for BDNF trophic support after axotomy is summa-
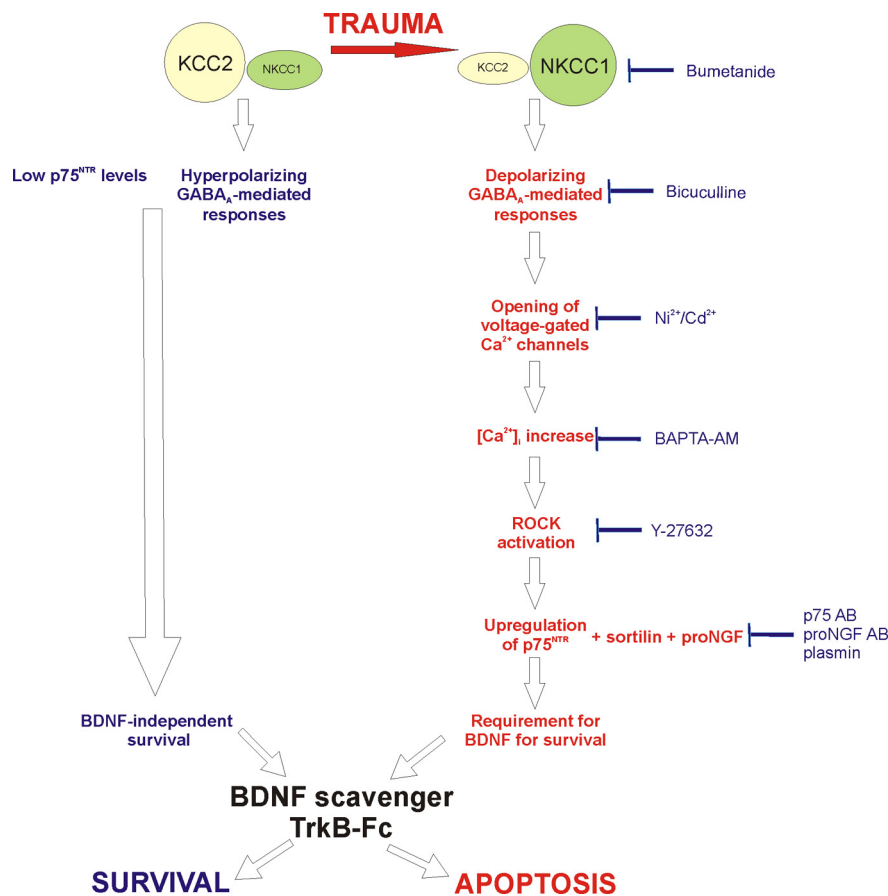
Figure 13. Proposed mechanism of the emergence of trauma-induced dependency on BDNF.

rized in Figure 13. The responses to axonal injury in the present *ex vivo* model strongly correlate to responses in several *in vivo* models studied in this and other works. Thus, this study justifies further preclinical and clinical studies on the therapeutic potential of bumetanide for injured neurons. According to our results, neuronal, neurotrophin-dependent survival after trauma can be profoundly affected by pharmacological agents acting on the GABAergic system and not on the neurotrophin system itself. This opens the possibility of developing more novel and well tolerated treatments than local supply of neurotrophic factors. On the basis of our results, bumetanide can be proposed as a potential treatment for the adult injured CNS. Notably, administration of GABA$_A$ agonists ethanol, benzodiazepines, and barbiturates to neonatal rats during the period of developmental synaptogenesis triggers widespread neuronal apoptosis (Ikonomidou et al., 2000): thus, in the future, understanding not only posttraumatic but also developmental coupling of GABA$_A$-mediated depolarization and p75^{NTR} expression could be of clinical significance.

References

Blaesse P, Airaksinen MS, Rivera C, Kaila K (2009) Cation-chloride cotransporters and neuronal function. Neuron 61:820–838.

Carlstedt T (2008) Root repair review: basic science background and clinical outcome. Restor Neurol Neurosci 26:225–241.

Chao MV (2003) Neurotrophins and their receptors: a convergence point for many signalling pathways. Nat Rev Neurosci 4:299–309.

Conner JM, Lauterborn JC, Yan Q, Gall CM, Varon S (1997) Distribution of brain-derived neurotrophic factor (BDNF) protein and mRNA in the normal adult rat CNS: evidence for anterograde axonal transport. J Neurosci 17:2295–2313.

Dechant G, Barde YA (2002) The neurotrophin receptor p75^{NTR}: novel functions and implications for diseases of the nervous system. Nat Neurosci 5:1131–1136.

Dhanoa NK, Krol KM, Jahed A, Crutcher KA, Kawaja MD (2006) Null mutations for exon III and exon IV of the p75 neurotrophin receptor gene enhance sympathetic sprouting in response to elevated levels of nerve growth factor in transgenic mice. Exp Neurol 198:416–426.

Dubreuil CI, Winton MJ, McKerracher L (2003) Rho activation patterns after spinal cord injury and the role of activated rho in apoptosis in the central nervous system. J Cell Biol 162:233–243.

Farrant M, Kaila K (2007) The cellular, molecular and ionic basis of GABA$_A$ receptor signalling. Prog Brain Res 160:59–87.

Gao X, Daugherty RL, Tourtellotte WG (2007) Regulation of low affinity neurotrophin receptor (p75^{NTR}) by early growth response (egr) transcriptional regulators. Mol Cell Neurosci 36:501–514.

Gehler S, Gallo G, Veien E, Letourneau PC (2004) p75 neurotrophin receptor signaling regulates growth cone filopodial dynamics through modulating RhoA activity. J Neurosci 24:4363–4372.

Giehl KM, Tetzlaff W (1996) BDNF and NT-3, but not NGF, prevent axotomy-induced death of rat corticospinal neurons in vivo. Eur J Neurosci 8:1167–1175.

Giehl KM, Röhrig S, Bonatz H, Gutjahr M, Leiner B, Bartke I, Yan Q, Reichardt LF, Backus C, Welcher AA, Dethleffsen K, Mestres P, Meyer M (2001) Endogenous brain-derived neurotrophic factor and neurotrophin-3 antagonistically regulate survival of axotomized corticospinal neurons in vivo. J Neurosci 21:3492–3502.

Harrington AW, Leiner B, Blechschmitt C, Arevalo JC, Lee R, Mörl K, Meyer M, Hempstead BL, Yoon SO, Giehl KM (2004) Secreted proNGF is a pathophysiological death-inducing ligand after adult CNS injury. Proc Natl Acad Sci U S A 101:6226–6230.

Huang EJ, Reichardt LF (2001) Neurotrophins: roles in neuronal development and function. Annu Rev Neurosci 24:677–736.

Huber LJ, Chao MV (1995) Mesenchymal and neuronal cell expression of the p75 neurotrophin receptor gene occur by different mechanisms. Dev Biol 167:227–238.

Ikonomidou C, Bittigau P, Ishimaru MJ, Wozniak DF, Koch C, Genz K, Price MT, Stefovska V, Hörster F, Tenkova T, Dikranian K, Olney JW (2000) Ethanol-induced apoptotic neurodegeneration and fetal alcohol syndrome. Science 287:1056–1060.

Jansen P, Giehl K, Nyengaard JR, Teng K, Lioubinski O, Sjoegaard SS, Breiderhoff T, Gotthardt M, Lin F, Eilers A, Petersen CM, Lewin GR, Hempstead BL, Willnow TE, Nykjaer A (2007) Roles for the proneurotrophin receptor sortilin in neuronal development, aging and brain injury. Nat Neurosci 10:1449–1457.

Klöcker N, Kermer P, Weishaupt JH, Labes M, Ankerhold R, Bähr M (2000) Brain-derived neurotrophic factor-mediated neuroprotection of adult rat retinal ganglion cells *in vivo* does not exclusively depend on phosphatidyl-inositol-3′-kinase/protein kinase B signaling. J Neurosci 20:6962–6967.

Lee HH, Jurd R, Moss SJ (2010) Tyrosine phosphorylation regulates the membrane trafficking of the potassium chloride co-transporter KCC2. Mol Cell Neurosci 45:173–179.

Lee KF, Li E, Huber LJ, Landis SC, Sharpe AH, Chao MV, Jaenisch R (1992) Targeted mutation of the gene encoding the low affinity NGF receptor p75 leads to deficits in the peripheral sensory nervous system. Cell 69:737–749.

Lee R, Kermani P, Teng KK, Hempstead BL (2001) Regulation of cell survival by secreted proneurotrophins. Science 294:1945–1948.

Li Y, Luikart BW, Birnbaum S, Chen J, Kwon CH, Kernie SG, Bassel-Duby R, Parada LF (2008) TrkB regulates hippocampal neurogenesis and governs sensitivity to antidepressive treatment. Neuron 59:399–412.

Liu C, Zuo J, Pertens E, Helli PB, Janssen LJ (2005) Regulation of Rho/ROCK signaling in airway smooth muscle by membrane potential and $[Ca^{2+}]_i$. Am J Physiol Lung Cell Mol Physiol 289:L574–L582.

Logue SE, Martin SJ (2008) Caspase activation cascades in apoptosis. Biochem Soc Trans 36:1–9.

Ludwig A, Li H, Saarma M, Kaila K, Rivera C (2003) Developmental up-regulation of KCC2 in the absence of GABAergic and glutamatergic transmission. Eur J Neurosci 18:3199–3206.

Maekawa M, Ishizaki T, Boku S, Watanabe N, Fujita A, Iwamatsu A, Obinata T, Ohashi K, Mizuno K, Narumiya S (1999) Signaling from rho to the actin cytoskeleton through protein kinases ROCK and LIM-kinase. Science 285:895–898.

Matsumoto T, Rauskolb S, Polack M, Klose J, Kolbeck R, Korte M, Barde YA (2008) Biosynthesis and processing of endogenous BDNF: CNS neurons store and secrete BDNF, not pro-BDNF. Nat Neurosci 11:131–133.

McKerracher L, Higuchi H (2006) Targeting rho to stimulate repair after spinal cord injury. J Neurotrauma 23:309–317.

Nabekura J, Ueno T, Okabe A, Furuta A, Iwaki T, Shimizu-Okabe C, Fukuda A, Akaike N (2002) Reduction of KCC2 expression and GABA_A receptor-mediated excitation after in vivo axonal injury. J Neurosci 22:4412–4417.

Pace AJ, Lee E, Athirakul K, Coffman TM, O'Brien DA, Koller BH (2000) Failure of spermatogenesis in mouse lines deficient in the Na^+-K^+-$2Cl^-$ cotransporter. J Clin Invest 105:441–450.

Peterson S, Bogenmann E (2003) Osmotic swelling induces p75 neurotrophin receptor (p75NTR) expression via nitric oxide. J Biol Chem 278:33943–33950.

Pfeffer CK, Stein V, Keating DJ, Maier H, Rinke I, Rudhard Y, Hentschke M, Rune GM, Jentsch TJ, Hübner CA (2009) NKCC1-dependent GABAergic excitation drives synaptic network maturation during early hippocampal development. J Neurosci 29:3419–3430.

Ramos A, Ho WC, Forte S, Dickson K, Boutilier J, Favell K, Barker PA (2007) Hypo-osmolar stress induces p75NTR expression by activating Sp1-dependent transcription. J Neurosci 27:1498–1506.

Rauskolb S, Zagrebelsky M, Dreznjak A, Deogracias R, Matsumoto T, Wiese S, Erne B, Sendtner M, Schaeren-Wiemers N, Korte M, Barde YA (2010) Global deprivation of brain-derived neurotrophic factor in the CNS reveals an area-specific requirement for dendritic growth. J Neurosci 30:1739–1749.

Risling M, Fried K, Lindå H, Cullheim S, Meier M (1992) Changes in nerve growth factor receptor-like immunoreactivity in the spinal cord after ventral funiculus lesion in adult cats. J Neurocytol 21:79–93.

Sakurada S, Takuwa N, Sugimoto N, Wang Y, Seto M, Sasaki Y, Takuwa Y (2003) Ca^{2+}-dependent activation of rho and rho kinase in membrane depolarization-induced and receptor stimulation-induced vascular smooth muscle contraction. Circ Res 93:548–556.

Schäbitz WR, Sommer C, Zoder W, Kiessling M, Schwaninger M, Schwab S (2000) Intravenous brain-derived neurotrophic factor reduces infarct size and counterregulates bax and bcl-2 expression after temporary focal cerebral ischemia. Stroke 31:2212–2217.

Shulga A, Thomas-Crusells J, Sigl T, Blaesse A, Mestres P, Meyer M, Yan Q, Kaila K, Saarma M, Rivera C, Giehl KM (2008) Posttraumatic GABA_A-mediated $[Ca^{2+}]_i$ increase is essential for the induction of brain-derived neurotrophic factor-dependent survival of mature central neurons. J Neurosci 28:6996–7005.

Shulga A, Blaesse A, Kysenius K, Huttunen HJ, Tanhuanpää K, Saarma M, Rivera C (2009) Thyroxin regulates BDNF expression to promote survival of injured neurons. Mol Cell Neurosci 42:408–418.

Song W, Volosin M, Cragnolini AB, Hempstead BL, Friedman WJ (2010) ProNGF induces PTEN via p75NTR to suppress trk-mediated survival signaling in brain neurons. J Neurosci 30:15608–15615.

Stoppini L, Buchs PA, Muller D (1991) A simple method for organotypic cultures of nervous tissue. J Neurosci Methods 37:173–182.

Thoenen H, Sendtner M (2002) Neurotrophins: from enthusiastic expectations through sobering experiences to rational therapeutic approaches. Nat Neurosci 5 [Suppl]:1046–1050.

Troy CM, Friedman JE, Friedman WJ (2002) Mechanisms of p75-mediated death of hippocampal neurons. Role of caspases. J Biol Chem 277:34295–34302.

Underwood CK, Coulson EJ (2008) The p75 neurotrophin receptor. Int J Biochem Cell Biol 40:1664–1668.

Volosin M, Song W, Almeida RD, Kaplan DR, Hempstead BL, Friedman WJ (2006) Interaction of survival and death signaling in basal forebrain neurons: roles of neurotrophins and proneurotrophins. J Neurosci 26:7756–7766.

Wang X, Bauer JH, Li Y, Shao Z, Zetoune FS, Cattaneo E, Vincenz C (2001) Characterization of a $p75^{NTR}$ apoptotic signaling pathway using a novel cellular model. J Biol Chem 276:33812–33820.

Weskamp G, Reichardt LF (1991) Evidence that biological activity of NGF is mediated through a novel subclass of high affinity receptors. Neuron 6:649–663.

Willems E, Mateizel I, Kemp C, Cauffman G, Sermon K, Leyns L (2006) Selection of reference genes in mouse embryos and in differentiating human and mouse ES cells. Int J Dev Biol 50:627–635.

Willnow TE, Petersen CM, Nykjaer A (2008) VPS10P-domain receptors—regulators of neuronal viability and function. Nat Rev Neurosci 9:899–909.

Yang J, Siao CJ, Nagappan G, Marinic T, Jing D, McGrath K, Chen ZY, Mark W, Tessarollo L, Lee FS, Lu B, Hempstead BL (2009) Neuronal release of proBDNF. Nat Neurosci 12:113–115.